



Weak decays of bottom-charm baryons: $\mathcal{B}_{bc} \rightarrow \mathcal{B}_b P$

Jia-Jie Han^{1,2,a}, Rui-Xiang Zhang^{1,b}, Hua-Yu Jiang^{2,3,c}, Zhen-Jun Xiao^{1,d}, Fu-Sheng Yu^{4,5,6,2,e}

¹ Department of Physics and Institute of Theoretical Physics, Nanjing Normal University, Nanjing 210023, Jiangsu, China

² School of Nuclear Science and Technology, Lanzhou University, Lanzhou 730000, China

³ Theoretische Physik 1, Naturwissenschaftlich-Technische Fakultät, Universität Siegen, 57068 Siegen, Germany

⁴ Lanzhou Center for Theoretical Physics, Lanzhou University, Lanzhou 730000, Gansu, China

⁵ Frontier Science Center for Rare Isotopes, Lanzhou University, Lanzhou 730000, China

⁶ Center for High Energy Physics, Peking University, Beijing 100871, China

Received: 31 January 2021 / Accepted: 10 May 2021 / Published online: 23 June 2021

© The Author(s) 2021

Abstract After the discovery of the double-charm baryon Ξ_{cc}^{++} by LHCb, one of the most important topics is to search for the bottom-charm baryons which contain a b quark, a c quark and a light quark. In this work, we study the two-body non-leptonic weak decays of a bottom-charm baryon into a spin-1/2 baryon and a light pseudoscalar meson with the short-distance contributions calculated under the factorization hypothesis and the long-distance contributions considering the final-state-interaction effects. The branching fractions of all fifty-seven decay channels are estimated. The results indicate that $\Xi_{bc}^+ \rightarrow \Xi_b^0 \pi^+$, $\Xi_{bc}^0 \rightarrow \Xi_b^- \pi^+$ and $\Omega_{bc}^0 \rightarrow \Omega_b^- \pi^+$ decay modes have relatively large decay rates and thus could be used to experimentally search for the bottom-charm baryons. The topological diagrams and the SU(3) symmetry of bottom-charm baryon decays are discussed.

1 Introduction

The recent discovery of the double-charm baryon Ξ_{cc}^{++} by the LHCb collaboration [1, 2] is the first observation of the double-heavy-flavor baryons which contain two heavy-flavor quarks (b or c) and one light quark (u , d or s) [3–5]. It opens a new window to understand the perturbative and non-perturbative features of the strong interaction, since their structure of two heavy quarks in the core and one light quark in the cloud is different from all the observed hadrons. It is natural and important to extend our studies to search for the

bottom-charm baryons ($\mathcal{B}_{bc} = \Xi_{bc}^+$, Ξ_{bc}^0 or Ω_{bc}^0). The heavy diquark core of bc could be somewhere different from that of cc .

The theoretical predictions on the branching fractions of weak decays of the bottom-charm baryons are very helpful for the experimental searches, analogous to the case of the observation of the double-charm baryon. There are too many decaying modes of heavy flavor hadrons. The experimental measurements prefer the modes with the largest branching fractions and easily detected final particles. In [6], it is suggested to search for the doubly charmed baryons via $\Xi_{cc}^{++} \rightarrow \Lambda_c^+ K^- \pi^+ \pi^+$ and $\Xi_{cc}^{++} \rightarrow \Xi_c^+ \pi^+$. Subsequently, the LHCb collaboration successfully observed Ξ_{cc}^{++} through the above suggested processes [1, 2]. The importance of theoretical studies on the weak decays is discussed in [7, 8].

The charm-quark decays dominate the decay rates of the bottom-charm baryons, like the B_c meson. It is known that around 70% decay rates of B_c comes from charm decays, 20% from b quark decays and 10% from $b\bar{c}$ annihilation. The large fractions from charm are induced by the dominate weak transitions of $c \rightarrow s$ with $|V_{cs}| \sim 1$, while the bottom decays are suppressed by $b \rightarrow c$ with $|V_{cb}| \sim 4 \times 10^{-2}$. Therefore, in this work, we will study the charm decays of the \mathcal{B}_{bc} baryons in order to point out the most favorable modes for experimental searches.

The dynamics of the non-leptonic charm decays are usually difficult to be calculated due to the large non-perturbative contributions at the charm scale [9–11]. In the recent years, the weak decays of charmed baryon decays have been extensively studied [12–38], as well as the weak decays of double-charm or bottom-charm baryons [39–65]. In [6], the non-leptonic decay amplitudes of the double-charm baryons are calculated with the factorizable contributions using the factorization approach and the non-factorizable contribution considering the rescattering mechanism of the final-state-

^a e-mail: hanjjie1020@163.com

^b e-mail: 854474645@qq.com

^c e-mail: jianghy15@lzu.edu.cn

^d e-mail: xiaozhenjun@njnu.edu.cn

^e e-mail: yufsh@lzu.edu.cn (corresponding author)

interaction effects. The observation of Ξ_{cc}^{++} via the processes predicted by the above theoretical framework manifests that it is reliable for charm decays of double-heavy baryons. This method has been systematically used to study the decays of double-charm baryon (\mathcal{B}_{cc}) into one charmed baryon and one pseudoscalar meson ($\mathcal{B}_c P$) [8], one charmed baryon and one vector meson ($\mathcal{B}_c V$) [40], and one light octet baryon and one charmed meson ($\mathcal{B} D^{(*)}$) [41]. In this work, we will use the same method to study the bottom-charm baryon decaying into one b -baryon and one light pseudoscalar meson, $\mathcal{B}_{bc} \rightarrow \mathcal{B}_b P$.

This paper is organized as follows. In Sect. 2, we describe theoretical framework adopted in this work. The numerical results and some discussions are collected in Sect. 3. Summary is in Sect. 4.

2 Theoretical framework

The effective Hamiltonian describes the tree-level charm decays is given by:

$$\mathcal{H}_{eff} = \frac{G_F}{\sqrt{2}} \sum_{q'=d,s} V_{cq'}^* V_{uq} [C_1(\mu) O_1(\mu) + C_2(\mu) O_2(\mu)] + h.c., \tag{1}$$

where $V_{cq'}^*$ and V_{uq} are CKM matrix elements, O_1 and O_2 are two four-fermion local operators:

$$\begin{aligned} O_1 &= (\bar{u}_\alpha q_\beta)_{V-A} (\bar{q}'_\beta c_\alpha)_{V-A}, \\ O_2 &= (\bar{u}_\alpha q_\alpha)_{V-A} (\bar{q}'_\beta c_\beta)_{V-A}, \end{aligned} \tag{2}$$

with $C_{1,2}$ as the relevant Wilson coefficients.

Comparing with the charm-quark decay of B_c meson, the weak decay of bc baryons can receive more complicated contributions even at the tree level. These contributions can be divided into several topological diagrams which are depicted in Fig. 1. T denotes color-favored W -external emission diagram. Different from the weak decay of meson which only receive one color-suppressed contribution and one W -exchange contribution, the baryon decays have two color-suppressed diagrams, denoted by C and C' in Fig. 1, and three W -exchange diagrams described by E_1 , E_2 and B . The difference between these topological diagrams is from the source of the quarks of the final-state hadrons. For example, the two quarks of the meson of the C diagram are both from the weak vertex, while the meson in the C' diagram is formed by one spectator quark and one quark from the weak vertex. With the analysis on the hierarchy, the topological diagram in charmed baryon decays are almost at the same order [66,67]. In the following, we will introduce our framework how to calculate each topological diagrams, for the short-distance and long-distance contributions, respectively.

2.1 Short-distance contributions under the factorization hypothesis

In the calculation of the short-distance contributions, T -topological diagram is considered as the dominating contribution which can be calculated under the factorization hypothesis. The short-distance contributions of the C diagram is negligible due to its smallness compared to T diagram.

The amplitude of $\mathcal{B}_{bc} \rightarrow \mathcal{B}_b P$ can be evaluated using the hadronic transition matrix elements:

$$\langle \mathcal{B}_b P | \mathcal{H}_{eff} | \mathcal{B}_{bc} \rangle = \frac{G_F}{\sqrt{2}} V_{cq'}^* V_{uq} \sum_{i=1,2} C_i \langle \mathcal{B}_b P | O_i | \mathcal{B}_{bc} \rangle. \tag{3}$$

According to the factorization hypothesis, the matrix elements $\langle \mathcal{B}_b P | O_i | \mathcal{B}_{bc} \rangle$ can be factorized into a product of two parts, the decay constants and the heavy-light transition form factors. The color-favored short-distance topological amplitude of the considered $\mathcal{B}_{bc} \rightarrow \mathcal{B}_b P$ weak decays can be expressed as:

$$\begin{aligned} &\langle \mathcal{B}_b M | \mathcal{H}_{eff} | \mathcal{B}_{bc} \rangle_{SD}^T \\ &= \frac{G_F}{\sqrt{2}} V_{cq'}^* V_{uq} a_1(\mu) \langle M | \bar{u} \gamma^\mu (1 - \gamma_5) q | 0 \rangle \\ &\quad \times \langle \mathcal{B}_b | \bar{q}' \gamma_\mu (1 - \gamma_5) c | \mathcal{B}_{bc} \rangle. \end{aligned} \tag{4}$$

Here, we also give the color-suppressed topology amplitude for convenience:

$$\begin{aligned} &\langle \mathcal{B}_b M | \mathcal{H}_{eff} | \mathcal{B}_{bc} \rangle_{SD}^C \\ &= \frac{G_F}{\sqrt{2}} V_{cq'}^* V_{uq} a_2(\mu) \langle M | \bar{q}' \gamma^\mu (1 - \gamma_5) q | 0 \rangle \\ &\quad \times \langle \mathcal{B}_b | \bar{u} \gamma_\mu (1 - \gamma_5) c | \mathcal{B}_{bc} \rangle, \end{aligned} \tag{5}$$

where $a_1(a_2)$ represents the effective Wilson coefficients, and $a_1(\mu) = C_1(\mu) + C_2(\mu)/3$ for the color-favored and $a_2(\mu) = C_2(\mu) + C_1(\mu)/3$ for the color-suppressed tree W -emission amplitudes, with the Wilson coefficients $C_1(\mu) = 1.21$ and $C_2(\mu) = -0.42$ at the typical scale of charm decays $\mu = m_c = 1.3$ GeV [10].

In Eqs. (4) and (5), the last matrix elements can be parameterized into six form factors:

$$\begin{aligned} &\langle \mathcal{B}_b(p', s'_2) | q' \gamma_\mu (1 - \gamma_5) c | \mathcal{B}_{bc}(p, s_z) \rangle \\ &= \bar{u}(p', s'_2) \left[\gamma_\mu f_1(q^2) + i \sigma_{\mu\nu} \frac{q^\nu}{M_{\mathcal{B}_{bc}}} f_2(q^2) \right. \\ &\quad \left. + \frac{q^\mu}{M_{\mathcal{B}_{bc}}} f_3(q^2) \right] u(p, s_z) \\ &\quad - \bar{u}(p', s'_2) \left[\gamma_\mu g_1(q^2) + i \sigma_{\mu\nu} \frac{q^\nu}{M_{\mathcal{B}_{bc}}} g_2(q^2) \right. \\ &\quad \left. + \frac{q^\mu}{M_{\mathcal{B}_{bc}}} g_3(q^2) \right] \gamma_5 u(p, s_z), \end{aligned} \tag{6}$$

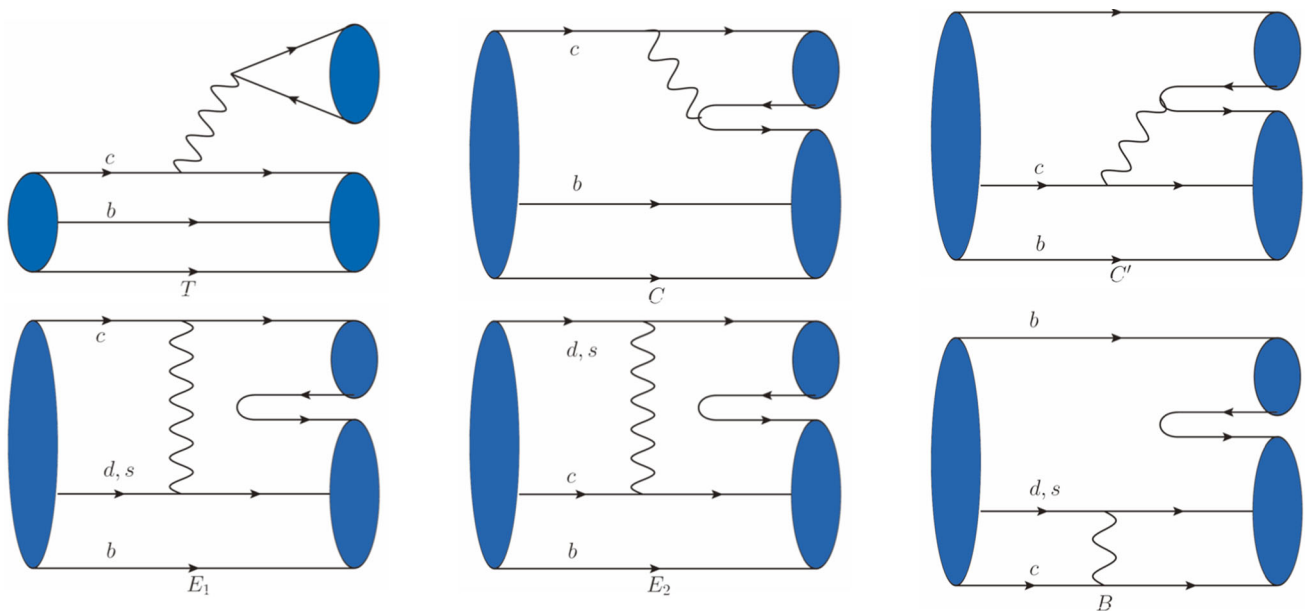


Fig. 1 Tree level topological diagrams for two body nonleptonic decays $\mathcal{B}_{bc} \rightarrow \mathcal{B}_b P$ of the bottom-charm baryons $\mathcal{B}_{bc} = (\Xi_{bc}^{+,0}, \Omega_{bc}^0)$

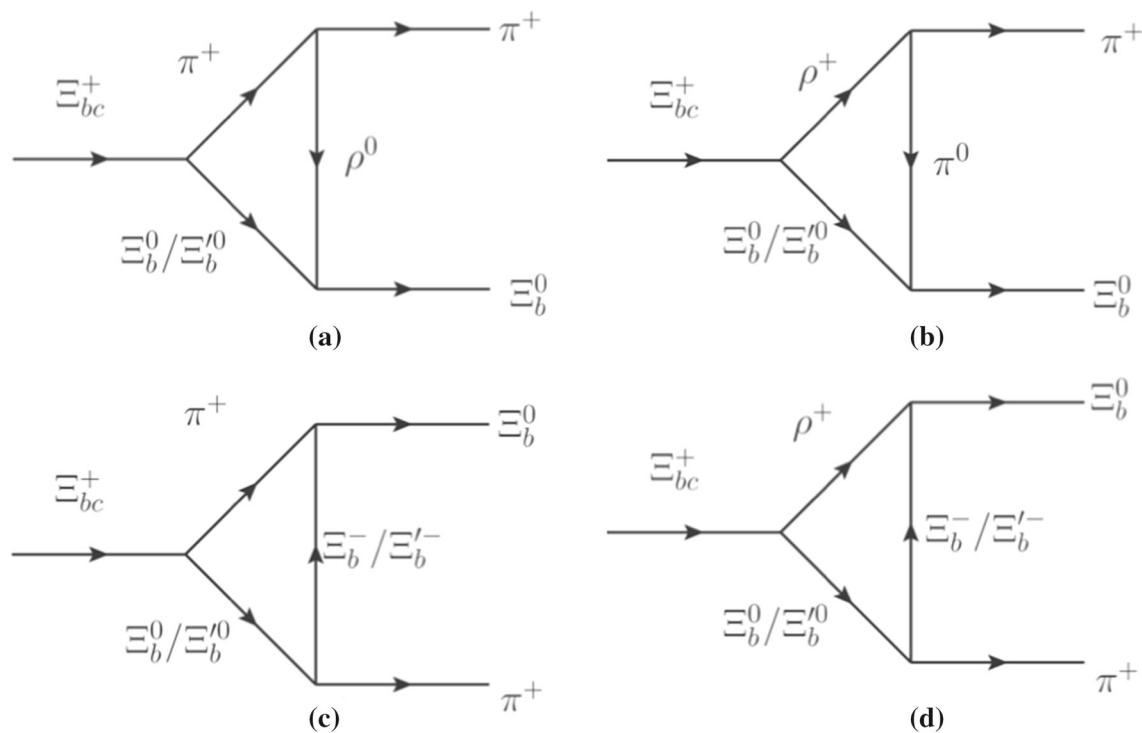


Fig. 2 The long-distance rescattering contributions to $\Xi_{bc}^+ \rightarrow \Xi_b^0 \pi^+$ at hadron level

with $q = p - p'$ and $M_{\mathcal{B}_{bc}}$ as the mass of \mathcal{B}_{bc} . The form factors f_i and g_i can be evaluated under different theoretical models.

The first matrix elements in Eqs. (4) and (5) are defined as decay constants:

$$\langle P(p) | \bar{u} \gamma^\mu (1 - \gamma_5) q | 0 \rangle = -i f_P p^\mu, \tag{7}$$

$$\langle V(p) | \bar{u} \gamma^\mu (1 - \gamma_5) q | 0 \rangle = m_V f_V \epsilon^{*\mu}, \tag{8}$$

where P is a pseudoscalar meson, and V a vector meson, and ϵ^μ represents the polarization vector of the vector meson. Combining Eqs. (4–8), the short-distance factorizable ampli-

tudes of $\mathcal{B}_{bc} \rightarrow \mathcal{B}_b P$ are:

$$\mathcal{A}_{SD}(\mathcal{B}_{bc} \rightarrow \mathcal{B}_b P) = i\bar{u}_{\mathcal{B}_b}(A + B\gamma_5)u_{\mathcal{B}_{bc}}, \tag{9}$$

$$\begin{aligned} \mathcal{A}_{SD}(\mathcal{B}_{bc} \rightarrow \mathcal{B}_b V) = \epsilon^{*\mu}\bar{u}_{\mathcal{B}_b} \left[A_1\gamma_\mu\gamma_5 + A_2\frac{p_\mu(\mathcal{B}_b)}{M_{\mathcal{B}_{bc}}}\gamma_5 \right. \\ \left. + B_1\gamma_\mu + B_2\frac{p_\mu(\mathcal{B}_b)}{M_{\mathcal{B}_{bc}}}\right] u_{\mathcal{B}_{bc}}, \end{aligned} \tag{10}$$

where the parameters A, B and $A_{1,2}, B_{1,2}$ usually include the whole information of strong interaction. In the factorization hypothesis, these parameters are expressed as

$$\begin{aligned} A &= \lambda f_P(M_{\mathcal{B}_{bc}} - M_{\mathcal{B}_b})f_1(m^2), \\ B &= \lambda f_P(M_{\mathcal{B}_{bc}} + M_{\mathcal{B}_b})g_1(m^2), \end{aligned} \tag{11}$$

$$\begin{aligned} A_1 &= -\lambda f_V m \left(g_1(m^2) + g_2(m^2)\frac{M_{\mathcal{B}_{bc}} - M_{\mathcal{B}_b}}{M_{\mathcal{B}_{bc}}} \right), \\ A_2 &= -2\lambda f_V m g_2(m^2), \end{aligned} \tag{12}$$

$$\begin{aligned} B_1 &= \lambda f_V m \left(f_1(m^2) - f_2(m^2)\frac{M_{\mathcal{B}_{bc}} + M_{\mathcal{B}_b}}{M_{\mathcal{B}_{bc}}} \right), \\ B_2 &= 2\lambda f_V m f_2(m^2), \end{aligned} \tag{13}$$

where $\lambda = \frac{G_F}{\sqrt{2}} V_{CKM} a_{1,2}(\mu)$, m is the mass of pseudoscalar or vector meson. V_{CKM} stands for the product of the two relevant CKM matrix elements.

2.2 Long-distance contributions from the rescattering mechanism

It is well known that the long-distance contributions are large in the charm decays. The most important problem in charmed hadron weak decays is to calculate the long-distance contributions. The C diagram is dominated by the long-distance contribution, since its short-distance contribution is negligible. The C', E_1, E_2 and B diagrams are absolutely contributed by the long-distance effects. We will calculate all these topological diagrams. As stated in the Introduction, we consider the rescattering mechanism of the FSI effects in this work.

The final-state interactions can be modeled as the rescattering of two intermediate particles at the hadronic level and described by the single-particle-exchange rescattering diagrams under the hadron-level strong effective Lagrangian. Taking the decay of $\Xi_{bc}^+ \rightarrow \Xi_b^0\pi^+$ as an example, the long-distance contributions come from all the $\Xi_{bc}^+ \rightarrow (\Xi_b^0/\Xi_b^{\prime 0})\pi^+ \rightarrow \Xi_b^0\pi^+$ and $\Xi_{bc}^+ \rightarrow (\Xi_b^0/\Xi_b^{\prime 0})\rho^+ \rightarrow \Xi_b^0\pi^+$ processes, as shown in Fig. 2. At present consideration, the intermediate states include the light pseudoscalar meson, vector mesons, and the ground anti-triplet and sextet bottom baryons.

The first weak transition vertex only involves the short-distance contributions calculated in the factorization hypothesis,

avoiding the double-counting problem. The following scattering process can be evaluated with hadronic strong effective Lagrangian. The theoretical framework is explained in detail in [8].

Now we will take the diagram Fig. 2b, $\Xi_{bc}^+ \rightarrow (\Xi_b^0/\Xi_b^{\prime 0})\rho^+ \rightarrow \Xi_b^0\pi^+$ with a π^0 exchanged, as a concrete example to explain calculation of this triangle diagrams. We adopt the optical theorem and Cutkosky cutting rule as in Ref. [68]. The absorptive part of this decay amplitude is calculated as

$$\begin{aligned} \text{Abs}[\mathcal{M}(P_{\Xi_{bc}^+} \rightarrow P_\pi + P_{\Xi_b^0})] \\ = \frac{1}{2} \int \frac{d^3 p_{\rho^+}}{(2\pi)^3 2E_1} \int \frac{d^3 p_{\Xi_b^0/\Xi_b^{\prime 0}}}{(2\pi)^3 2E_2} (2\pi)^4 \delta^4(p_{\pi^+} \\ + p_{\Xi_b^0} - p_{\rho^+} - p_{\Xi_b^0/\Xi_b^{\prime 0}}) \\ \cdot M(P_{\Xi_{bc}^+} \rightarrow (\Xi_b^0/\Xi_b^{\prime 0})\rho^+) T^*(\pi^+ \Xi_b^0 \rightarrow (\Xi_b^0/\Xi_b^{\prime 0})\rho^+). \end{aligned} \tag{14}$$

The amplitudes of the weak vertex $\Xi_{bc}^+ \rightarrow (\Xi_b^0/\Xi_b^{\prime 0})\rho^+$ are taken from Eq. (10). The rescattering amplitudes of $(\Xi_b^0/\Xi_b^{\prime 0})\rho^+ \rightarrow \Xi_b^0\pi^+$ can be simply carried out from the hadronic strong-interaction Lagrangian in Appendix A. Then substituting the two parts into Eq. (14), the absorptive part is written as:

$$\begin{aligned} \text{Abs}[\mathcal{M}(\rho^+, \Xi_b^0; \pi^0)] \\ = \int \frac{|\vec{p}_1| \sin\theta d\theta d\phi}{32\pi^2 m_{\Xi_{bc}^+}} (-ig_{\rho^+\pi^0\pi^-}) ig_{\Xi_b^0\pi^0\Xi_b^0} \bar{u}(p_4, s_4) i\gamma_5 (\not{p}_2 + m_2) \\ \times \frac{F^2(t, m_k)}{t - m_k^2 + im_k\Gamma_k} \\ \cdot \left(\left(-2\not{p}_3 + \frac{2p_3 \cdot p_1 \not{p}_1}{m_1^2} \right) (A_1\gamma_5 + B_1) \right. \\ \left. + \frac{-2m_1^2 p_3 \cdot p_2 + 2p_3 \cdot p_1 p_1 \cdot p_2}{m_1^2 m_{\Xi_{bc}^+}} (A_2\gamma_5 + B_2) \right) u(p_i, s_i), \end{aligned} \tag{15}$$

$$\begin{aligned} \text{Abs}[\mathcal{M}(\rho^+, \Xi_b^{\prime 0}; \pi^0)] \\ = \int \frac{|\vec{p}_1| \sin\theta d\theta d\phi}{32\pi^2 m_{\Xi_{bc}^+}} (-ig_{\rho^+\pi^0\pi^-}) ig_{\Xi_b^{\prime 0}\pi^0\Xi_b^{\prime 0}} \bar{u}(p_4, s_4) i\gamma_5 (\not{p}_2 + m_2) \\ \times \frac{F^2(t, m_k)}{t - m_k^2 + im_k\Gamma_k} \\ \cdot \left(\left(-2\not{p}_3 + \frac{2p_3 \cdot p_1 \not{p}_1}{m_1^2} \right) (A_1\gamma_5 + B_1) \right. \\ \left. + \frac{-2m_1^2 p_3 \cdot p_2 + 2p_3 \cdot p_1 p_1 \cdot p_2}{m_1^2 m_{\Xi_{bc}^+}} (A_2\gamma_5 + B_2) \right) u(p_i, s_i), \end{aligned} \tag{16}$$

where $t = p_{\pi^0}^2$. The subscript i denotes the initial state Ξ_{bc}^+ , while 1, 2 and k represent the intermediate states $\rho^+, (\Xi_b^0/\Xi_b^{\prime 0})$ and π^0 , and 3, 4 for the final states π^+ and Ξ_b^0 , respectively. In our calculation, the exchanged π^0 is generally off-shell, which means the strong coupling constants in the rescattering process are not exactly correct and need to be modified. To account for the off-shell effect of π^0 , a form

factor $F(t, m_\pi)$ is introduced [68] as

$$F(t, m_\pi) = \frac{\Lambda^2 - m_\pi^2}{\Lambda^2 - t}, \tag{17}$$

normalized to unity at the on-shell point $t = p_k^2 = m_\pi^2$. The cutoff Λ has the form of

$$\Lambda = m_\pi + \eta \Lambda_{\text{QCD}}, \tag{18}$$

with $\Lambda_{\text{QCD}} = 330$ MeV for charm decays. The phenomenological parameter η can not be calculated from the first-principle methods, and usually needs to be determined by the experimental data. The final results are usually sensitive to the value of η . More discussions about η can be found in Sect. 3.

The dispersive part can be calculated by the dispersion relation of

$$\text{Dis}[A(m_1^2)] = \frac{1}{\pi} \int_s^\infty \frac{\text{Abs}[A(s')]}{s' - m_1^2} ds', \tag{19}$$

which suffers from large ambiguities [68]. The integration in Eq.(19) depends on the knowledge of $\text{Abs}[A(s')]$ in a very large region from s to infinity, which is unavailable currently. Therefore, it is difficult to evaluate how large the dispersive part is. In charm decays as discussed in [6, 8, 68], the hadronic triangle diagrams would be dominated by the absorptive part, since the total masses of final states are not far from, if not close to, the initial charmed hadrons, especially for charmed baryon decays. In phenomenology, the non-zero dispersive part are absorbed into the only free parameter η . As η can not be calculated from the first principles, it would be finally determined by the experimental data. Then, such effects as the dispersive parts are all involved in the determination of η , but expected not to affect η too much. Besides, the dispersive part mainly affect the studies of CP violations which are sensitive to the strong phases of amplitudes. In the studies of branching fractions, it can be safely involved into the effects of η .

By the same approach mentioned in the above section, the absorptive amplitude of the rest triangle diagrams in Fig. 2 can be carried out as:

$$\begin{aligned} \text{Abs}[\mathcal{M}(\pi^+, \Xi_b^0; \rho^0)] &= \int \frac{|\bar{p}_1| \sin\theta d\theta d\phi}{32\pi^2 m_{\Xi_{bc}^+}} i^2 (-ig_{\pi^+\rho^0\pi^-}) \\ &\times \frac{F^2(t, m_{\rho^0})}{t - m_{\rho^0}^2 + im_{\rho^0}\Gamma_{\rho^0}} \bar{u}(p_4, s_4) \\ &\cdot \left[f_{1\Xi_b^0\rho^0\Xi_b^0} (-\eta_1 - \eta_3) \right. \\ &+ \frac{k \cdot (p_1 + p_3) \not{k}}{m_{\rho^0}^2} \left. \right] \\ &+ \frac{f_{2\Xi_b^0\rho^0\Xi_b^0}}{2m_{\Xi_b^0}} (-\not{k}(\eta_1 + \eta_3) + k \cdot (p_1 + p_3)) \left. \right] \\ &\cdot (\eta_2 + m_2)(A + B\gamma_5)u(p_i, s_i), \end{aligned} \tag{20}$$

$$\begin{aligned} \text{Abs}[\mathcal{M}(\pi^+, \Xi_b^0; \rho^0)] &= \int \frac{|\bar{p}_1| \sin\theta d\theta d\phi}{32\pi^2 m_{\Xi_{bc}^+}} i^2 (-ig_{\pi^+\rho^0\pi^-}) \\ &\times \frac{F^2(t, m_{\rho^0})}{t - m_{\rho^0}^2 + im_{\rho^0}\Gamma_{\rho^0}} \\ &\cdot \bar{u}(p_4, s_4) \left(f_{1\Xi_b^0\rho^0\Xi_b^0} (-\eta_1 - \eta_3) \right. \\ &+ \frac{k \cdot (p_1 + p_3) \not{k}}{m_{\rho^0}^2} \left. \right) \\ &+ \frac{f_{2\Xi_b^0\rho^0\Xi_b^0}}{m_{\Xi_b^0} + m_{\Xi_b^0}} (-\not{k}(\eta_1 + \eta_3) + k \cdot (p_1 + p_3)) \\ &\cdot (\eta_2 + m_2)(A + B\gamma_5)u(p_i, s_i), \end{aligned} \tag{21}$$

$$\begin{aligned} \text{Abs}[\mathcal{M}(\pi^+, \Xi_b^0; \Xi_b^-)] &= \int \frac{|\bar{p}_1| \sin\theta d\theta d\phi}{32\pi^2 m_{\Xi_{bc}^+}} ig_{\pi^+\Xi_b^-\Xi_b^0} g_{\Xi_b^0\Xi_b^-\pi^-} \bar{u} \\ &(p_3, s_3) \gamma_5 (\not{k} + m_k) \gamma_5 (\eta_2 + m_2) \\ &\cdot (A + B\gamma_5)u(p_i, s_i) \\ &\times \frac{F^2(t, m_{\Xi_b^-})}{t - m_{\Xi_b^-}^2 + im_{\Xi_b^-}\Gamma_{\Xi_b^-}}, \end{aligned} \tag{22}$$

$$\begin{aligned} \text{Abs}[\mathcal{M}(\pi^+, \Xi_b^0; \Xi_b'^-)] &= \int \frac{|\bar{p}_1| \sin\theta d\theta d\phi}{32\pi^2 m_{\Xi_{bc}^+}} ig_{\pi^+\Xi_b'^-\Xi_b^0} g_{\Xi_b^0\Xi_b'^-\pi^-} \bar{u} \\ &(p_3, s_3) \gamma_5 (\not{k} + m_k) \gamma_5 (\eta_2 + m_2) \\ &\cdot (A + B\gamma_5)u(p_i, s_i) \\ &\times \frac{F^2(t, m_{\Xi_b'^-})}{t - m_{\Xi_b'^-}^2 + im_{\Xi_b'^-}\Gamma_{\Xi_b'^-}}, \end{aligned} \tag{23}$$

$$\begin{aligned} \text{Abs}[\mathcal{M}(\pi^+, \Xi_b^0; \Xi_b^-)] &= \int \frac{|\bar{p}_1| \sin\theta d\theta d\phi}{32\pi^2 m_{\Xi_{bc}^+}} ig_{\pi^+\Xi_b^-\Xi_b^0} g_{\Xi_b^0\Xi_b^-\pi^-} \bar{u} \\ &(p_3, s_3) \gamma_5 (\not{k} + m_k) \gamma_5 (\eta_2 + m_2) \\ &\cdot (A + B\gamma_5)u(p_i, s_i) \\ &\times \frac{F^2(t, m_{\Xi_b^-})}{t - m_{\Xi_b^-}^2 + im_{\Xi_b^-}\Gamma_{\Xi_b^-}}, \end{aligned} \tag{24}$$

$$\begin{aligned} \text{Abs}[\mathcal{M}(\pi^+, \Xi_b^0; \Xi_b'^-)] &= \int \frac{|\bar{p}_1| \sin\theta d\theta d\phi}{32\pi^2 m_{\Xi_{bc}^+}} ig_{\pi^+\Xi_b'^-\Xi_b^0} g_{\Xi_b^0\Xi_b'^-\pi^-} \bar{u} \\ &(p_3, s_3) \gamma_5 (\not{k} + m_k) \gamma_5 (\eta_2 + m_2) \\ &\cdot (A + B\gamma_5)u(p_i, s_i) \\ &\times \frac{F^2(t, m_{\Xi_b'^-})}{t - m_{\Xi_b'^-}^2 + im_{\Xi_b'^-}\Gamma_{\Xi_b'^-}}, \end{aligned} \tag{25}$$

$$\begin{aligned} \text{Abs}[\mathcal{M}(\rho^+, \Xi_b^0; \Xi_b^-)] &= \int \frac{|\bar{p}_1| \sin\theta d\theta d\phi}{32\pi^2 m_{\Xi_{bc}^+}} i^3 \bar{u}(p_3, s_3) \\ &\left(f_{1\rho^+\Xi_b^-\Xi_b^0} \gamma_\nu - \frac{if_{2\rho^+\Xi_b^-\Xi_b^0}}{m_k + m_3} \sigma_{\mu\nu} P_1^\mu \right) g_{\Xi_b^0\Xi_b^-\pi^+} \\ &\cdot (\not{k} + m_k) \frac{F^2(t, m_{\Xi_b^-})}{t - m_{\Xi_b^-}^2 + im_{\Xi_b^-}\Gamma_{\Xi_b^-}} \gamma_5 \left(-g^{\nu\alpha} \right. \\ &+ \frac{P_1^\nu P_1^\alpha}{m_1^2} \left. \right) (\eta_2 + m_2) \\ &\cdot \left(A_1 \gamma_\alpha \gamma_5 + A_2 \frac{P_2^\alpha}{m_{bc}^+} \gamma_5 + B_1 \gamma_\alpha \right. \\ &+ \left. B_2 \frac{P_2^\alpha}{m_{bc}^+} \right) u(p_i, s_i), \end{aligned} \tag{26}$$

$$\begin{aligned} \text{Abs}[\mathcal{M}(\rho^+, \Xi_b^0; \Xi_b'^-)] &= \int \frac{|\bar{p}_1| \sin\theta d\theta d\phi}{32\pi^2 m_{\Xi_{bc}^+}} i^3 \bar{u}(p_3, s_3) \\ &\left(f_{1\rho^+\Xi_b'^-\Xi_b^0} \gamma_\nu - \frac{if_{2\rho^+\Xi_b'^-\Xi_b^0}}{m_k + m_3} \sigma_{\mu\nu} P_1^\mu \right) g_{\Xi_b^0\Xi_b'^-\pi^+} \end{aligned}$$

$$\begin{aligned}
 & \cdot (\not{k} + m_k) \frac{F^2(t, m_{\Xi_b^-})}{t - m_{\Xi_b^-}^2 + im_{\Xi_b^-} \Gamma_{\Xi_b^-}} \gamma_5 \left(-g^{v\alpha} \right. \\
 & \left. + \frac{p_1^\nu p_1^\alpha}{m_1^2} \right) (\not{p}_2 + m_2) \\
 & \cdot \left(A_1 \gamma_\alpha \gamma_5 + A_2 \frac{p_{2\alpha}}{m_{bc}^+} \gamma_5 \right. \\
 & \left. + B_1 \gamma_\alpha + B_2 \frac{p_{2\alpha}}{m_{bc}^+} \right) u(p_i, s_i), \tag{27}
 \end{aligned}$$

$$\begin{aligned}
 Abs[\mathcal{M}(\rho^+, \Xi_b^0; \Xi_b^-)] &= \int \frac{|\bar{p}_1| \sin\theta d\theta d\phi}{32\pi^2 m_{\Xi_b^+}} i^3 \bar{u}(p_3, s_3) \\
 & \left(f_{1\rho^+ \Xi_b^- \Xi_b^0} \gamma_\nu \right. \\
 & \left. - \frac{if_{2\rho^+ \Xi_b^- \Xi_b^0}}{m_k + m_3} \sigma_{\mu\nu} p_1^\mu \right) g_{\Xi_b^0 \Xi_b^- \pi^+} \\
 & \cdot (\not{k} + m_k) \frac{F^2(t, m_{\Xi_b^-})}{t - m_{\Xi_b^-}^2 + im_{\Xi_b^-} \Gamma_{\Xi_b^-}} \gamma_5 \left(-g^{v\alpha} \right. \\
 & \left. + \frac{p_1^\nu p_1^\alpha}{m_1^2} \right) (\not{p}_2 + m_2) \\
 & \cdot \left(A_1 \gamma_\alpha \gamma_5 + A_2 \frac{p_{2\alpha}}{m_{bc}^+} \gamma_5 \right. \\
 & \left. + B_1 \gamma_\alpha + B_2 \frac{p_{2\alpha}}{m_{bc}^+} \right) u(p_i, s_i), \tag{28}
 \end{aligned}$$

$$\begin{aligned}
 Abs[\mathcal{M}(\rho^+, \Xi_b^0; \Xi_b^-)] &= \int \frac{|\bar{p}_1| \sin\theta d\theta d\phi}{32\pi^2 m_{\Xi_b^+}} i^3 \bar{u}(p_3, s_3) \\
 & \left(f_{1\rho^+ \Xi_b^- \Xi_b^0} \gamma_\nu - \frac{if_{2\rho^+ \Xi_b^- \Xi_b^0}}{m_k + m_3} \sigma_{\mu\nu} p_1^\mu \right) g_{\Xi_b^0 \Xi_b^- \pi^+} \\
 & \cdot (\not{k} + m_k) \frac{F^2(t, m_{\Xi_b^-})}{t - m_{\Xi_b^-}^2 + im_{\Xi_b^-} \Gamma_{\Xi_b^-}} \gamma_5 \left(-g^{v\alpha} \right. \\
 & \left. + \frac{p_1^\nu p_1^\alpha}{m_1^2} \right) (\not{p}_2 + m_2) \\
 & \cdot \left(A_1 \gamma_\alpha \gamma_5 + A_2 \frac{p_{2\alpha}}{m_{bc}^+} \gamma_5 \right. \\
 & \left. + B_1 \gamma_\alpha + B_2 \frac{p_{2\alpha}}{m_{bc}^+} \right) u(p_i, s_i). \tag{29}
 \end{aligned}$$

Collecting all the amplitudes together, the total amplitude of $\Xi_{bc} \rightarrow \Xi_b^0 \pi^+$ is expressed as:

$$\begin{aligned}
 \mathcal{A}(\Xi_{bc}^+ \rightarrow \Xi_b^0 \pi^+) &= \mathcal{T}_{SD}(\Xi_{bc}^+ \rightarrow \Xi_b^0 \pi^+) \\
 & + i Abs \left[\mathcal{M}(\pi^+, \Xi_b^0; \rho^0) + \mathcal{M}(\pi^+, \Xi_b^0; \rho^0) \right. \\
 & + \mathcal{M}(\rho^+, \Xi_b^0; \pi^0) + \mathcal{M}(\rho^+, \Xi_b^0; \pi^0) \\
 & + \mathcal{M}(\pi^+, \Xi_b^0; \Xi_b^-) + \mathcal{M}(\pi^+, \Xi_b^0; \Xi_b^-) \\
 & + \mathcal{M}(\pi^+, \Xi_b^0; \Xi_b^-) + \mathcal{M}(\pi^+, \Xi_b^0; \Xi_b^-) \\
 & + \mathcal{M}(\rho^+, \Xi_b^0; \Xi_b^-) + \mathcal{M}(\rho^+, \Xi_b^0; \Xi_b^-) \\
 & \left. + \mathcal{M}(\rho^+, \Xi_b^0; \Xi_b^-) + \mathcal{M}(\rho^+, \Xi_b^0; \Xi_b^-) \right], \tag{30}
 \end{aligned}$$

where \mathcal{T}_{SD} stands for the short-distance contributions of topological diagram T . The amplitudes of all the other channels for bc baryons decaying have been collected into Appendix 1.

Table 1 Masses (in units of GeV) and lifetime (in units of fs) of the bottom-charmed baryons considered in this paper, as given in Refs. [69, 70]

Baryons	Ξ_{bc}^+	Ξ_{bc}^0	Ω_{bc}^0
Masses	6.94	6.94	7.02
Lifetime	240	220	180

3 Numerical results and discussions

For the calculation of the branching ratios, we need to know all inputs used in this work. For lack of experimental data, we use the theoretical results of the masses and lifetimes from Ref. [69, 70] as shown in Table 1. For the bottom-charm baryons, there are two sets of SU(3) triplets, Ξ_{bc}, Ω_{bc} and Ξ'_{bc}, Ω'_{bc} . Those two triplets have different J^P for the heavy di-quark system bc . Only the lighter ones can weak decay with sizable branching fractions. The theoretical results obtained in Ref. [69] show that bc-baryons with $J^P = 1^+$ are the lighter ones.

The lifetimes are an important feature to calculate the branching fractions and in the experimental measurements [7]. They are also calculated in [49] that $409\text{fs} < \tau(\Xi_{bc}^+) < 607\text{fs}$, $93\text{fs} < \tau(\Xi_{bc}^0) < 118\text{fs}$, $168\text{fs} < \tau(\Omega_{bc}^0) < 370\text{fs}$. Compared to those in [70], it can be found that the current status of predictions on the lifetimes of bottom-charm baryons are of large ambiguity, due to the special role of charm. It has to keep in mind that the final results of branching fractions are proportional to the lifetimes. Our following results could be naively replaced by some other values of lifetimes.

The masses and the decay constants of the final-state particles are from [71–73]. The transition form factors in Eq. (6) have been computed out by several methods. We will use the results calculated by the light-front quark model [45] as inputs, which have been successfully used in the prediction of the discovery channel $\Xi_{cc}^{++} \rightarrow \Lambda_c^+ K^- \pi^+ \pi^+$ and $\Xi_c^+ \pi^+$ in [6]. Strong coupling constants can be found in the literatures [74–79], and the unfound ones are calculated with respect to the SU(3) symmetry. The strong coupling constants appeared in our calculation are gathered in the Appendix 1.

The branching ratios of the decay modes $\mathcal{B}_{bc} \rightarrow \mathcal{B}_b P$ are listed in Tables 2, 3, 4 and 5. According to the characteristic of the relevant CKM matrix elements for a given decay mode, all decay modes can be classified into 4 classes: the short-distance contribution dominated processes in Table 2, and the long-distance contribution dominated processes of the Cabibbo-favored (CF) decays induced by $c \rightarrow s u \bar{d}$ in Table 3, the singly Cabibbo-suppressed (SCS) ones induced by $c \rightarrow d u \bar{d}$ or $c \rightarrow s u \bar{s}$ in Table 4, and the doubly Cabibbo-suppressed (DCS) ones induced by $c \rightarrow d u \bar{s}$ in Table 5. In those tables, the topological amplitudes of each decay mode are listed at the third column with $\lambda_{sd} = V_{cs}^* V_{ud}$, $\lambda_{ds} = V_{cd}^* V_{us}$, $\lambda_d = V_{cd}^* V_{ud}$ and $\lambda_s = V_{cs}^* V_{us}$. The *tilde* is used to distinguish the channels with sextet bottom-baryons in the final state, from the ones without *tilde* for the anti-

triplet bottom baryons. The branching fractions that involve the long-distance contributions corresponding to three different values of η , i.e. $\eta=1.0, 1.5$ and 2.0 , are listed at the fifth, sixth and seventh column, respectively.

The sensitivity of branching ratios to the parameter η in Eq. (17) has already been demonstrated in Refs. [6, 40]. Taking the decay channels of $\mathcal{B}_{bc}^+ \rightarrow \Sigma_b^- \bar{K}^0$ and $\mathcal{B}_{bc}^0 \rightarrow \Lambda_b^0 \bar{K}^0$ as an example shown in Fig. 3a, we can find that the branching fractions can be changed by almost one order of magnitude for η varying from 1 to 2. As pointed out in [6, 8], however, the ratios of branching fractions are insensitive to η , seen in Fig. 3b. Apparently, the ratio is changed very slightly with the variation of η . The large uncertainty from the η is mostly canceled in the ratio of branching fractions. This behavior helps us to improve the prediction power.

One can see in Table 2 that the short-distance contributions of the external W-emission T diagrams, T_{SD} , are the dominant contributions to the modes including it. However, the long-distance dynamics dominate the decay modes without the T diagrams, which can be easily read out from Tables 3, 4 and 5. For comparison, we display the short-distance contribution of the internal W-emission C diagram under the factorization hypothesis, C_{SD} , at the fourth column in Tables 3, 4 and 5. It is found that C_{SD} are much smaller than triangle diagram contributions. The reason is that the effective Wilson coefficient $a_2(\mu)$ at the charm mass scale is deeply suppressed, $a_2(m_c) = -0.017$.

Considering the non-factorizable contributions in the color-suppressed tree-emission diagram, C , it is convenient to parameterize such effects in the effective Wilson coefficients $a_{1,2}^{\text{eff}}(\mu) = C_{1,2}(\mu) + C_{2,1}(\mu)/N_c^{\text{eff}}$ [80]. The values of $a_{1,2}^{\text{eff}}(\mu)$ are actually process dependent. In charmed meson decays, it is found that $|a_2^{\text{eff}}/a_1^{\text{eff}}| \sim 0.6 - 0.8$ and $\arg(a_2^{\text{eff}}/a_1^{\text{eff}}) \sim 110^\circ - 170^\circ$ which are obtained from the global fits for the topological amplitudes [9, 10], where the uncertainties are well under control due to the precise measurements of branching fractions. In this work, the non-factorizable effects are modeled by the rescattering mechanism whose uncertainties are characterized by the parameter η . Since there are not available data currently, we could not determine the value of η very well. Varying η from 1 to 2, the results could be changed by one order of magnitude for the processes dominated by the non-factorizable effects.

In the same CKM mode, decays with T_{SD} contributions tend to have largest branching fractions. Under our theoretical framework, T_{SD} is absolutely the dominating contribution comparing to the non-factorizable contributions. As a result, one can see from the Table 2 that branching ratios receiving T_{SD} contributions are not sensitive to the variation of η . However, the picture is totally different for the other types of contributions which increase or decrease rapidly as η changes, which indicates important FSI effects.

Our results can be compared to those in the previous literatures. Branching ratios of two non-leptonic decay modes of Ξ_{bc} baryon are estimated under NRQCD sum rules in Ref. [81], i.e. $\mathcal{B}r(\Xi_{bc}^+ \rightarrow \Xi_b^0 \pi^+) = 7.7\%$ and $\mathcal{B}r(\Xi_{bc}^0 \rightarrow \Xi_b^- \pi^+) = 7.1\%$, which is almost twice as what we predicted. This deviation is mainly caused by the weak transition form factors. The form factors used in our work are $f_1 = 0.627$ and $g_1 = 0.167$ for both decay modes, while $f_1 \sim g_1 \sim 0.9$ are employed in Ref. [81]. With the form factors calculated in the light-front quark model, Ref. [45] estimates the branching ratios of the \mathcal{T} -topological diagram involving processes in the factorization approach. Their results are very close to ours, since the form factors used in this work are taken from Ref. [45]. Besides, the \mathcal{T} -topological diagrams are the dominant contributions in this kind of decay modes. Thus the rescattering effects don't affect the total branching fractions very much.

In Ref. [6], the process of $\Xi_{cc}^{++} \rightarrow \Xi_c^+ \pi^+$ is recommended as a discovery channel of Ξ_{cc}^{++} , which has been confirmed by the LHCb experiment in Ref. [2]. Similarly here, we suggest the LHCb collaboration to search for the bottom-charm baryons by the modes of $\Xi_{bc}^+ \rightarrow \Xi_b^0 \pi^+$, $\Xi_{bc}^0 \rightarrow \Xi_b^- \pi^+$ and $\Omega_{bc}^0 \rightarrow \Omega_b^- \pi^+$, respectively, who have the relatively larger branching ratios. The branching ratios of those three decays are given as:

$$\mathcal{B}R(\Xi_{bc}^+ \rightarrow \Xi_b^0 \pi^+) = (3.50 \sim 3.95)\%, \tag{31}$$

$$\mathcal{B}R(\Xi_{bc}^0 \rightarrow \Xi_b^- \pi^+) = (3.15 \sim 3.32)\%, \tag{32}$$

$$\mathcal{B}R(\Omega_{bc}^0 \rightarrow \Omega_b^- \pi^+) = 2.54\%. \tag{33}$$

With the branching fractions of $\Xi_{bc}^+ \rightarrow \Sigma_b^+ \bar{K}^0$ and $\Xi_{bc}^+ \rightarrow \Xi_b^0 \pi^+$ in Tables 2 and 3, we calculate the ratio between long-distance contribution of topological diagram C and short-distance contribution of T with $\eta = 1.0 \sim 2.0$,

$$\frac{|\mathcal{A}(\Xi_{bc}^+ \rightarrow \Sigma_b^+ \bar{K}^0)|}{|\mathcal{A}(\Xi_{bc}^+ \rightarrow \Xi_b^0 \pi^+)|} \approx \frac{C_{LD}}{T_{SD}} \approx 0.2 \sim 0.44 \tag{34}$$

In Table 3, there are three channels only include one kind of topological diagrams, i.e. $\Xi_{bc}^+ \rightarrow \Sigma_b^+ \bar{K}^0$, $\Xi_{bc}^0 \rightarrow \Omega_b^- K^+$ and $\Xi_{bc}^0 \rightarrow \Sigma_b^+ K^-$. They are more convenient for the studies on the topological diagrams. Although, we can extract the absolute value of the corresponding topological diagram amplitude, the ratios between these amplitudes have a more important sense. Our numerical results are

$$\frac{|\mathcal{A}(\Xi_{bc}^0 \rightarrow \Sigma_b^+ K^-)|}{|\mathcal{A}(\Xi_{bc}^+ \rightarrow \Sigma_b^+ \bar{K}^0)|} = \frac{|E_1|}{|C|} = 0.69 \sim 0.86, \tag{35}$$

$$\frac{|\mathcal{A}(\Xi_{bc}^0 \rightarrow \Omega_b^- K^+)|}{|\mathcal{A}(\Xi_{bc}^+ \rightarrow \Sigma_b^+ \bar{K}^0)|} = \frac{|E_2|}{|C|} = 0.52 \sim 0.59. \tag{36}$$

Table 2 Branching ratios for the short-distance dominated modes. The ‘‘CF’’, ‘‘SCS’’ and ‘‘DCS’’ represent CKM favored, singly CKM suppressed and doubly CKM suppressed processes, respectively

Particles	Decay modes	Topology	$\mathcal{BR}_{T_{SD}}(\%)$	$\mathcal{BR}_{\eta=1.0}(\%)$	$\mathcal{BR}_{\eta=1.5}(\%)$	$\mathcal{BR}_{\eta=2.0}(\%)$	CKM
Ξ_{bc}^+	$\rightarrow \Xi_b^0 \pi^+$	$\lambda_{sd}(T + C')$	3.50	3.58	3.73	3.95	CF
	$\rightarrow \Xi_b^0 \pi^+$	$\frac{1}{\sqrt{2}}\lambda_{sd}(\tilde{T} + \tilde{C}')$	2.04	2.07	2.13	2.21	CF
	$\rightarrow \Sigma_b^0 \pi^+$	$\frac{1}{\sqrt{2}}\lambda_d(\tilde{T} + \tilde{C}')$	0.11	0.12	0.12	0.13	SCS
	$\rightarrow \Lambda_b^0 \pi^+$	$\lambda_d(T + C')$	0.21	0.22	0.23	0.25	SCS
	$\rightarrow \Xi_b^0 K^+$	$\frac{1}{\sqrt{2}}\lambda_s(\tilde{T} + \tilde{C}')$	0.14	0.14	0.15	0.15	SCS
	$\rightarrow \Xi_b^0 K^+$	$\lambda_s(T + C')$	0.30	0.31	0.33	0.35	SCS
	$\rightarrow \Lambda_b^0 K^+$	$\lambda_{ds}(T + C')$	0.019	0.020	0.020	0.021	DCS
	$\rightarrow \Sigma_b^0 K^+$	$\frac{1}{\sqrt{2}}\lambda_{ds}(\tilde{T} + \tilde{C}')$	0.0086	0.0087	0.0090	0.0094	DCS
Ξ_{bc}^0	$\rightarrow \Xi_b^- \pi^+$	$\lambda_{sd}(T - E_2)$	3.15	3.15	3.23	3.32	CF
	$\rightarrow \Xi_b^- \pi^+$	$\frac{1}{\sqrt{2}}\lambda_{sd}(\tilde{T} + \tilde{E}_2)$	1.84	1.85	1.86	1.89	CF
	$\rightarrow \Sigma_b^- \pi^+$	$\lambda_d(\tilde{T} + \tilde{E}_2)$	0.21	0.21	0.21	0.22	SCS
	$\rightarrow \Xi_b^- K^+$	$\frac{1}{\sqrt{2}}(\lambda_s \tilde{T} + \lambda_d \tilde{E}_2)$	0.13	0.13	0.13	0.13	SCS
	$\rightarrow \Xi_b^- K^+$	$\lambda_s T + \lambda_d E_2$	0.27	0.27	0.28	0.28	SCS
	$\rightarrow \Sigma_b^- K^+$	$\lambda_{ds} \tilde{T}$	0.016				DCS
Ω_{bc}^0	$\rightarrow \Omega_b^- \pi^+$	$\lambda_{sd} \tilde{T}$	2.54				CF
	$\rightarrow \Xi_b^- \pi^+$	$-\lambda_d T - \lambda_s E_2$	0.12	0.12	0.12	0.13	SCS
	$\rightarrow \Xi_b^- \pi^+$	$\frac{1}{\sqrt{2}}(\lambda_d \tilde{T} + \lambda_s \tilde{E}_2)$	0.071	0.072	0.072	0.073	SCS
	$\rightarrow \Omega_b^- K^+$	$\lambda_s(\tilde{T} + \tilde{E}_2)$	0.17	0.17	0.17	0.18	SCS
	$\rightarrow \Xi_b^- K^+$	$\lambda_{ds}(-T + E_2)$	0.011	0.011	0.011	0.011	DCS
	$\rightarrow \Xi_b^- K^+$	$\frac{1}{\sqrt{2}}\lambda_{ds}(\tilde{T} + \tilde{E}_2)$	0.0052	0.0052	0.0053	0.0054	DCS

We can see that the ratios $|E_1|/|C|$ and $|E_2|/|C|$ are all at the order one, confirmed to the result in [66]. Similarly, the ratios can also be obtained from Table 4,

$$\frac{|\mathcal{A}(\Xi_{bc}^0 \rightarrow \Sigma_b^+ \pi^-)|}{|\mathcal{A}(\Xi_{bc}^+ \rightarrow \Sigma_b^+ \pi^0)|} = \frac{|E_1|}{|C|} = 0.55 \sim 0.62, \tag{37}$$

$$\frac{|\mathcal{A}(\Omega_{bc}^0 \rightarrow \Sigma_b^+ K^-)|}{|\mathcal{A}(\Xi_{bc}^+ \rightarrow \Sigma_b^+ \pi^0)|} = \frac{|E_1|}{|C|} = 0.56 \sim 0.58, \tag{38}$$

and from Table 5,

$$\frac{|\mathcal{A}(\Omega_{bc}^0 \rightarrow \Sigma_b^- \pi^+)|}{|\mathcal{A}(\Xi_{bc}^+ \rightarrow \Sigma_b^+ K^0)|} = \frac{|E_2|}{|C|} = 0.43 \sim 0.46, \tag{39}$$

$$\frac{|\mathcal{A}(\Omega_{bc}^0 \rightarrow \Sigma_b^+ \pi^-)|}{|\mathcal{A}(\Xi_{bc}^+ \rightarrow \Sigma_b^+ K^0)|} = \frac{|E_1|}{|C|} = 0.68 \sim 0.77. \tag{40}$$

It is clear that all the results are consistent within the theoretical uncertainties.

The C' diagram can be indirectly extracted from the channel with the topological amplitudes of $T + C'$ in Table 2. The

ratios between C' and C are given by:

$$\frac{|\mathcal{A}(\Xi_{bc}^+ \rightarrow \Xi_b^0 \pi^+)_{LD}|}{|\mathcal{A}(\Xi_{bc}^+ \rightarrow \Sigma_b^+ \bar{K}^0)|} = \frac{|C'|}{|C|} = 0.91 \sim 0.95, \tag{41}$$

$$\frac{|\mathcal{A}(\Xi_{bc}^+ \rightarrow \Lambda_b^0 \pi^+)_{LD}|}{|\mathcal{A}(\Xi_{bc}^+ \rightarrow \Sigma_b^+ \pi^0)|} = \frac{|C'|}{|C|} = 0.82 \sim 0.84, \tag{42}$$

$$\frac{|\mathcal{A}(\Xi_{bc}^+ \rightarrow \Xi_b^0 K^+)_{LD}|}{|\mathcal{A}(\Xi_{bc}^+ \rightarrow \Sigma_b^+ \pi^0)|} = \frac{|C'|}{|C|} = 0.99 \sim 1.03, \tag{43}$$

$$\frac{|\mathcal{A}(\Xi_{bc}^+ \rightarrow \Lambda_b^0 K^+)_{LD}|}{|\mathcal{A}(\Xi_{bc}^+ \rightarrow \Sigma_b^+ K^0)|} = \frac{|C'|}{|C|} = 0.97 \sim 1.0 \tag{44}$$

From Eqs. (34–44), we get the similar conclusion as in Refs. [66,67].

$$\frac{|C|}{|T|} \sim \frac{|C'|}{|C|} \sim \frac{|E_1|}{|C|} \sim \frac{|E_2|}{|C|} \sim O(\Lambda_{QCD}/m_c) \sim O(1). \tag{45}$$

In heavy quark decays, the flavor $SU(3)$ symmetry is a useful tool. A number of relations between decay widths are found within the $SU(3)$ symmetry [47]. To test the $SU(3)$ symmetry and its breaking, we show the ratios in our calculations in Eqs. (46–54). All of these ratios should be unity in

Table 3 Branching ratios for the long-distance dominated Cabibbo-favored modes. For the channels involving internal W-emission contributions, the short-distance factorizable contributions are also listed at the fourth column for comparison

Particles	Decay modes	Topology	$\mathcal{BR}_{T_{SD}} (\times 10^{-3})$	$\mathcal{BR}_{\eta=1.0} (\times 10^{-3})$	$\mathcal{BR}_{\eta=1.5} (\times 10^{-3})$	$\mathcal{BR}_{\eta=2.0} (\times 10^{-3})$
Ξ_{bc}^+ Ξ_{bc}^0	$\rightarrow \Sigma_b^+ \bar{K}^0$	\tilde{C}	7.88×10^{-3}	0.83	2.31	4.34
	$\rightarrow \Omega_b^- K^+$	\tilde{E}_2		0.15	0.55	1.01
	$\rightarrow \Sigma_b^0 \bar{K}^0$	$\frac{1}{\sqrt{2}}(\tilde{C} + \tilde{E}_1)$	7.07×10^{-3}	1.05	3.29	6.80
	$\rightarrow \Lambda_b^0 \bar{K}^0$	$-C + E_1$	8.42×10^{-3}	0.12	0.35	0.73
	$\rightarrow \Sigma_b^+ K^-$	\tilde{E}_1		0.36	1.28	2.89
	$\rightarrow \Xi_b^0 \pi^0$	$\frac{1}{2}(-\tilde{C}' + \tilde{E}_2)$	4.66×10^{-3}	0.24	0.73	1.48
	$\rightarrow \Xi_b^0 \eta_1$	$\frac{1}{\sqrt{6}}(\tilde{C}' + \tilde{E}_1 + \tilde{E}_2)$				
	$\rightarrow \Xi_b^0 \eta_8$	$\frac{1}{2\sqrt{3}}(\tilde{C}' - 2\tilde{E}_1 + \tilde{E}_2)$	5.96×10^{-3}	0.039	0.132	0.325
	$\rightarrow \Xi_b^0 \pi^0$	$-\frac{1}{\sqrt{2}}(C' + E_2)$	7.96×10^{-3}	1.00	2.89	5.62
	$\rightarrow \Xi_b^0 \eta_1$	$\frac{1}{\sqrt{3}}(C' + E_1 - E_2)$				
Ω_{bc}^0	$\rightarrow \Xi_b^0 \eta_8$	$\frac{1}{\sqrt{6}}(C' - 2E_1 - E_2)$		0.021	0.083	0.206
	$\rightarrow \Xi_b^0 \bar{K}^0$	$\frac{1}{\sqrt{2}}(\tilde{C} + \tilde{C}')$	6.34×10^{-3}	0.86	2.43	4.63
	$\rightarrow \Xi_b^0 \bar{K}^0$	$-C + C'$	7.33×10^{-3}	0.36	1.06	2.08

Table 4 The same as Table 3 but for singly Cabibbo-suppressed modes

Particles	Decay modes	Topology	$\mathcal{BR}_{T_{SD}} (\times 10^{-5})$	$\mathcal{BR}_{\eta=1.0} (\times 10^{-5})$	$\mathcal{BR}_{\eta=1.5} (\times 10^{-5})$	$\mathcal{BR}_{\eta=2.0} (\times 10^{-5})$
Ξ_{bc}^+	$\rightarrow \Sigma_b^+ \pi^0$	$-\frac{1}{\sqrt{2}} \tilde{C}$	4.65×10^{-2}	7.95	26.5	55.2
	$\rightarrow \Sigma_b^+ \eta_1$	$\frac{1}{\sqrt{3}} (\lambda_d + \lambda_s) \tilde{C}$				
	$\rightarrow \Sigma_b^+ \eta_8$	$\frac{1}{\sqrt{6}} (\lambda_d - 2\lambda_s) \tilde{C}$	4.10×10^{-2}	6.15	19.2	39.8
	$\rightarrow \Sigma_b^0 \pi^0$	$\frac{1}{2} \lambda_d (-\tilde{C} - \tilde{C}' + \tilde{E}_1 + \tilde{E}_2)$	5.19×10^{-2}	11.5	35.7	72.7
	$\rightarrow \Sigma_b^0 \eta_1$	$\frac{1}{\sqrt{6}} [\lambda_d (\tilde{C} + \tilde{C}' + \tilde{E}_1 + \tilde{E}_2) + \lambda_s \tilde{C}]$				
	$\rightarrow \Sigma_b^0 \eta_8$	$\frac{1}{2\sqrt{3}} [\lambda_d (\tilde{C} + \tilde{C}' + \tilde{E}_1 + \tilde{E}_2) - 2\lambda_s \tilde{C}]$	6.56×10^{-2}	6.30	20.3	43.5
	$\rightarrow \Lambda_b^0 \pi^0$	$\frac{1}{\sqrt{2}} \lambda_d (C - C' - E_1 - E_2)$	6.00×10^{-2}	9.81	31.6	66.3
	$\rightarrow \Lambda_b^0 \eta_1$	$\frac{1}{\sqrt{3}} [\lambda_d (C' - C + E_1 - E_2) - \lambda_s C]$				
	$\rightarrow \Lambda_b^0 \eta_8$	$\frac{1}{\sqrt{6}} [\lambda_d (C' - C + E_1 - E_2) + 2\lambda_s C]$	7.88×10^{-2}	0.139	3.70	6.83
	$\rightarrow \Sigma_b^+ \pi^-$	$\lambda_d \tilde{E}_1$				
Ω_{bc}^0	$\rightarrow \Xi_b^0 K^0$	$\frac{1}{\sqrt{2}} (\lambda_s \tilde{C}' + \lambda_d \tilde{E}_1)$	3.25×10^{-2}	2.18	8.01	18.6
	$\rightarrow \Xi_b^0 K^0$	$\lambda_s C' + \lambda_d E_1$	6.88×10^{-2}	0.66	2.44	5.88
	$\rightarrow \Sigma_b^0 \bar{K}^0$	$\frac{1}{\sqrt{2}} (\lambda_d \tilde{C}' + \lambda_s \tilde{E}_1)$	1.81×10^{-2}	2.92	7.7	13.8
	$\rightarrow \Lambda_b^0 \bar{K}^0$	$\lambda_d C' + \lambda_s E_1$	3.24×10^{-2}	0.82	2.60	5.60
	$\rightarrow \Sigma_b^+ K^-$	$\lambda_s \tilde{E}_1$				
	$\rightarrow \Xi_b^0 \pi^0$	$\frac{1}{2} (-\lambda_d \tilde{C} + \lambda_s \tilde{E}_2)$	1.80×10^{-2}	0.88	2.72	5.69
	$\rightarrow \Xi_b^0 \eta_1$	$\frac{1}{\sqrt{6}} [\lambda_s (\tilde{C} + \tilde{C}' + \tilde{E}_1 + \tilde{E}_2) + \lambda_d \tilde{C}]$				
	$\rightarrow \Xi_b^0 \eta_8$	$\frac{1}{2\sqrt{3}} [\lambda_s (\tilde{E}_2 - 2\tilde{C} - 2\tilde{C}' - 2\tilde{E}_1) + \lambda_d \tilde{C}]$	4.79×10^{-2}	8.92	28.0	58.3
	$\rightarrow \Xi_b^0 \pi^0$	$\frac{1}{\sqrt{2}} (\lambda_d C - \lambda_s E_2)$	3.060×10^{-2}	0.84	2.24	4.21
	$\rightarrow \Xi_b^0 \eta_1$	$\frac{1}{\sqrt{3}} [\lambda_s (C' - C + E_1 - E_2) - \lambda_d C]$				
$\rightarrow \Xi_b^0 \eta_8$	$\frac{1}{\sqrt{6}} [\lambda_s (2C - 2C' + 2E_1 - E_2) - \lambda_d C]$	6.82×10^{-3}	4.42	14.3	30.9	

Table 5 The same as Table 3 but for doubly Cabibbo-suppressed modes

Particles	Decay modes	Topology	$\mathcal{BR}_{T_{SD}} (\times 10^{-6})$	$\mathcal{BR}_{\eta=1.0} (\times 10^{-6})$	$\mathcal{BR}_{\eta=1.5} (\times 10^{-6})$	$\mathcal{BR}_{\eta=2.0} (\times 10^{-6})$
Ξ_{bc}^+	$\rightarrow \Sigma_b^+ K^0$	\tilde{C}	4.10×10^{-2}	2.50	7.69	15.8
Ξ_{bc}^0	$\rightarrow \Sigma_b^0 K^0$	$\frac{1}{\sqrt{2}}(\tilde{C} + \tilde{C}')$	3.91×10^{-2}	4.72	14.6	29.6
	$\rightarrow \Lambda_b^0 K^0$	$-C + C'$	4.65×10^{-2}	2.12	6.65	13.7
Ω_{bc}^0	$\rightarrow \Sigma_b^0 \pi^0$	$\frac{1}{2}(-\tilde{E}_1 + \tilde{E}_2)$		0.403	1.35	2.90
	$\rightarrow \Sigma_b^0 \eta_1$	$\frac{1}{\sqrt{6}}(\tilde{C}' + \tilde{E}_1 + \tilde{E}_2)$				
	$\rightarrow \Sigma_b^0 \eta_8$	$\frac{1}{2\sqrt{3}}(-2\tilde{C}' + \tilde{E}_1 + \tilde{E}_2)$	1.46×10^{-2}	0.53	1.63	3.40
	$\rightarrow \Lambda_b^0 \pi^0$	$-\frac{1}{\sqrt{2}}(E_1 + E_2)$		1.21	4.03	8.72
	$\rightarrow \Lambda_b^0 \eta_1$	$\frac{1}{\sqrt{3}}(C' + E_1 - E_2)$				
	$\rightarrow \Lambda_b^0 \eta_8$	$-\frac{1}{\sqrt{6}}(2C' - E_1 + E_2)$	3.10×10^{-2}	1.67	5.00	10.1
	$\rightarrow \Sigma_b^+ \pi^+$	\tilde{E}_2		0.395	1.31	2.92
	$\rightarrow \Sigma_b^+ \pi^-$	\tilde{E}_1		0.99	3.51	8.03
	$\rightarrow \Xi_b^0 K^0$	$\frac{1}{\sqrt{2}}(\tilde{C} + \tilde{E}_1)$	1.32×10^{-2}	2.55	8.59	18.9
	$\rightarrow \Xi_b^0 K^+$	$-C + E_1$	2.73×10^{-2}	0.408	1.04	2.01

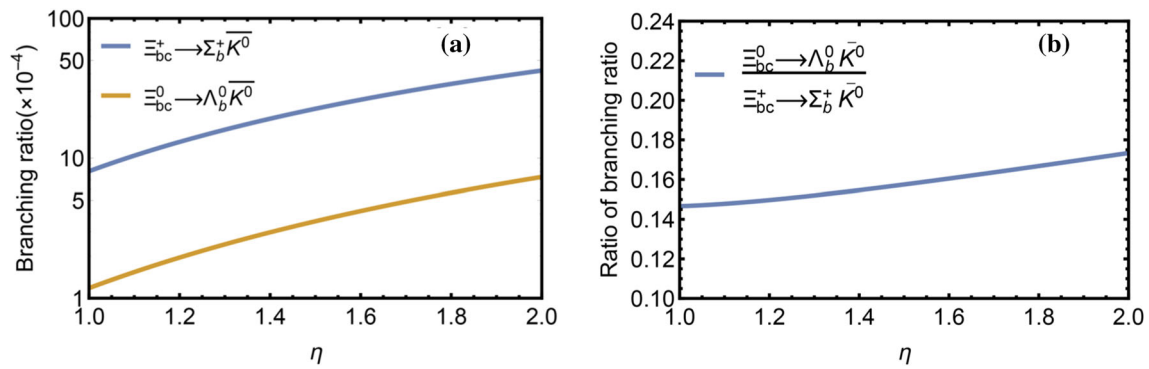


Fig. 3 **a** The theoretical predictions for the branching ratios of $\Xi_{bc}^+ \rightarrow \Sigma_b^+ K^0$ and $\Xi_{bc}^0 \rightarrow \Lambda_b^0 K^0$ in logarithmic coordinates. **b** ratio of branching fractions with η varying from 1.0 to 2.0

the $SU(3)$ limit. The corresponding topological amplitudes are given as well.

$$\Gamma(\Xi_{bc}^+ \rightarrow \Lambda_b^0 \pi^+) / \Gamma(\Xi_{bc}^+ \rightarrow \Xi_b^0 K^+) = |\lambda_d(T + C')|^2 / |\lambda_s(T + C')|^2 = 0.70 \sim 0.71, \tag{46}$$

$$\Gamma(\Xi_{bc}^0 \rightarrow \Xi_b^0 K^0) / \Gamma(\Omega_{bc}^0 \rightarrow \Lambda_b^0 \bar{K}^0) = |\lambda_s C' + \lambda_d E_1|^2 / |\lambda_d C' + \lambda_s E_1|^2 = 2.94 \sim 3.08, \tag{47}$$

$$\Gamma(\Omega_{bc}^0 \rightarrow \Xi_b^- \pi^+) / \Gamma(\Xi_{bc}^0 \rightarrow \Xi_b^- K^+) = |-\lambda_d T - \lambda_s E_2|^2 / |\lambda_s T + \lambda_d E_2|^2 = 0.58 \sim 0.59, \tag{48}$$

$$\Gamma(\Xi_{bc}^+ \rightarrow \Sigma_b^+ \pi^0) / \frac{1}{3} \Gamma(\Xi_{bc}^+ \rightarrow \Sigma_b^+ \eta_8) = |-\frac{1}{\sqrt{2}} \tilde{C}|^2 / |-\frac{1}{\sqrt{6}} (\lambda_d - 2\lambda_s) \tilde{C}|^2 = 5.89 \sim 6.57, \tag{49}$$

$$\Gamma(\Xi_{bc}^+ \rightarrow \Sigma_b^0 \pi^+) / \Gamma(\Xi_{bc}^+ \rightarrow \Xi_b^0 K^+) = |\frac{1}{\sqrt{2}} \lambda_d (\tilde{T} + \tilde{C}')|^2 / |\frac{1}{\sqrt{2}} \lambda_s (\tilde{T} + \tilde{C}')|^2 = 0.80 \sim 0.81, \tag{50}$$

$$\Gamma(\Xi_{bc}^0 \rightarrow \Sigma_b^+ \pi^-) / \Gamma(\Omega_{bc}^0 \rightarrow \Sigma_b^+ K^-) = |\lambda_d \tilde{E}_1|^2 / |\lambda_s \tilde{E}_1|^2 = 0.89 \sim 1.02, \tag{51}$$

$$\Gamma(\Xi_{bc}^0 \rightarrow \Sigma_b^- \pi^+) / \Gamma(\Omega_{bc}^0 \rightarrow \Omega_b^- K^+) = |\lambda_d (\tilde{T} + \tilde{E}_2)|^2 / |\lambda_s (\tilde{T} + \tilde{E}_2)|^2 = 0.90 \sim 0.91, \tag{52}$$

$$\Gamma(\Xi_{bc}^0 \rightarrow \Xi_b^0 K^0) / \Gamma(\Omega_{bc}^0 \rightarrow \Sigma_b^0 \bar{K}^0) = |\frac{1}{\sqrt{2}} (\lambda_s \tilde{C}' + \lambda_d \tilde{E}_1)|^2 / |\frac{1}{\sqrt{2}} (\lambda_d \tilde{C}' + \lambda_s \tilde{E}_1)|^2 = 0.60 \sim 0.77, \tag{53}$$

$$\Gamma(\Omega_{bc}^0 \rightarrow \Xi_b^- \pi^+) / \Gamma(\Xi_{bc}^0 \rightarrow \Xi_b^- K^+) = |\frac{1}{\sqrt{2}} (\lambda_d \tilde{T}' + \lambda_s \tilde{E}_2)|^2 / |\frac{1}{\sqrt{2}} (\lambda_s \tilde{T}' + \lambda_d \tilde{E}_2)|^2 = 0.38 \sim 0.72. \tag{54}$$

The above results indicate that the long-distance final-state interactions can contribute to large $SU(3)$ breaking effect. It would be of great help to research the $SU(3)$ symmetry in the heavy baryon decays in case that the long-distance dynamics can be calculated accurately.

4 Summary

In this work, we investigate the two-body non-leptonic weak decays of the bottom-charm baryons Ξ_{bc}^+ , Ξ_{bc}^0 and Ω_{bc}^0 with the long-distance contributions included. This long-distance contributions, which are non-perturbative and can not be calculated under factorization hypothesis, are viewed as the final-state-interactions in this paper. The rescattering mechanism has been adopted for the calculations.

This paper exhibit the calculated branching ratios that include all the processes $\mathcal{B}_{bc} \rightarrow \mathcal{B}_b P$. Based on our results of all fifty-seven decay modes considered in this, we recommend the three processes $\Xi_{bc}^+ \rightarrow \Xi_b^0 \pi^+$, $\Xi_{bc}^0 \rightarrow \Xi_b^- \pi^+$ and $\Omega_{bc}^0 \rightarrow \Omega_b^- \pi^+$ as the potentials of the discovery channels. The T topological diagrams are found to have the largest contribution. Short-distance factorizable contribution T_{SD} is dominating if one decay mode can receive T -topology contribution and the branching ratio of this type of decay mode is not sensitive to the variation of η . However, branching ratios with C_{SD} or purely nonfactorizable contributions vary rapidly as η changes while the ratio between any two branching fractions is almost independent of the variation of η .

We also calculate the ratios between different topological diagram, and find that in charm decay, the relations $\frac{|C|}{|T|} \sim \frac{|C'|}{|C|} \sim \frac{|E_1|}{|C|} \sim \frac{|E_2|}{|C|} \sim \mathcal{O}(\frac{\Lambda_{QCD}}{m_c}) \sim \mathcal{O}(1)$ are hold as declared in literatures [66,67]. The $SU(3)$ breaking effects between decay modes are calculated and some larger $SU(3)$ breaking decay modes have been found which have significant guidance for the following researches of bottom-charm baryon decays.

Acknowledgements This work was supported by the National Natural Science Foundation of China under the Grant nos. 11775117, U1732101, 11975112, and National Key Research and Development Program of China under Contracts no. 2020YFA0406400.

Data Availability Statement This manuscript has no associated data or the data will not be deposited. [Author’s comment: This is a theoretical study and no experimental data has been listed.]

Open Access This article is licensed under a Creative Commons Attribution 4.0 International License, which permits use, sharing, adaptation, distribution and reproduction in any medium or format, as long as you give appropriate credit to the original author(s) and the source, provide a link to the Creative Commons licence, and indicate if changes were made. The images or other third party material in this article are included in the article’s Creative Commons licence, unless indicated otherwise in a credit line to the material. If material is not included in the article’s Creative Commons licence and your intended use is not permitted by statutory regulation or exceeds the permitted use, you will need to obtain permission directly from the copyright holder. To view a copy of this licence, visit <http://creativecommons.org/licenses/by/4.0/>.
 Funded by SCOAP³.

Appendix A: Effective Lagrangians

The effective Lagrangians used in the rescattering mechanism are those as given in Refs. [74–78]:

$$\mathcal{L}_{VPP} = \frac{ig_{VPP}}{\sqrt{2}} Tr[V^\mu [P, \partial_\mu P]], \tag{A1}$$

$$\mathcal{L}_{VVV} = \frac{ig_{VVV}}{\sqrt{2}} Tr[(\partial_\nu V_\mu V^\mu - V^\mu \partial_\nu V_\mu) V^\nu], \tag{A2}$$

$$\mathcal{L}_{PB_6B_6} = g_{PB_6B_6} Tr[\bar{B}_6 i \gamma_5 P B_6], \tag{A3}$$

$$\mathcal{L}_{PB_3B_3} = g_{PB_3B_3} Tr[\bar{B}_3 i \gamma_5 P B_3], \tag{A4}$$

$$\mathcal{L}_{PB_6B_3} = g_{PB_6B_3} Tr[\bar{B}_6 i \gamma_5 P B_3] + h.c., \tag{A5}$$

$$\begin{aligned} \mathcal{L}_{VB_6B_6} = & f_{1VB_6B_6} Tr[\bar{B}_6 \gamma_\mu V^\mu B_6] \\ & + \frac{f_{2PB_6B_6}}{2m_6} Tr[\bar{B}_6 \sigma_{\mu\nu} \partial^\mu V^\nu B_6], \end{aligned} \tag{A6}$$

$$\begin{aligned} \mathcal{L}_{VB_3B_3} = & f_{1PB_3B_3} Tr[\bar{B}_3 \gamma_\mu V^\mu B_3] \\ & + \frac{f_{2PB_3B_3}}{2m_3} Tr[\bar{B}_3 \sigma_{\mu\nu} \partial^\mu V^\nu B_3], \end{aligned} \tag{A7}$$

$$\begin{aligned} \mathcal{L}_{VB_6B_3} = & \left\{ f_{1VB_6B_3} Tr[\bar{B}_6 \gamma_\mu V^\mu B_3] \right. \\ & \left. + \frac{f_{2VB_6B_3}}{m_6 + m_3} Tr[\bar{B}_6 \sigma_{\mu\nu} \partial^\mu V^\nu B_3] \right\} + h.c., \end{aligned} \tag{A8}$$

$$\begin{aligned} P(J^P = 0^-) = & \begin{pmatrix} \frac{\pi^0}{\sqrt{2}} + \frac{\eta_8}{\sqrt{6}} & \pi^+ & K^+ \\ \pi^- & -\frac{\pi^0}{\sqrt{2}} + \frac{\eta_8}{\sqrt{6}} & K^0 \\ K^- & \bar{K}^0 & -\sqrt{\frac{2}{3}}\eta_8 \end{pmatrix} \\ & + \frac{1}{\sqrt{3}} \begin{pmatrix} \eta_1 & 0 & 0 \\ 0 & \eta_1 & 0 \\ 0 & 0 & \eta_1 \end{pmatrix}, \end{aligned} \tag{A9}$$

$$\begin{aligned} V(J^P = 1^-) = & \begin{pmatrix} \frac{\rho^0}{\sqrt{2}} + \frac{\omega}{\sqrt{2}} & \rho^+ & K^{*+} \\ \rho^- & -\frac{\rho^0}{\sqrt{2}} + \frac{\omega}{\sqrt{2}} & K^{*0} \\ K^{*-} & \bar{K}^{*0} & \phi \end{pmatrix}, \end{aligned} \tag{A10}$$

$$\begin{aligned} B_6 \left(J^P = \frac{1}{2}^+ \right) = & \begin{pmatrix} \Sigma_b^+ & \frac{\Sigma_b^0}{\sqrt{2}} & \frac{\Xi_b^0}{\sqrt{2}} \\ \frac{\Sigma_b^0}{\sqrt{2}} & \Sigma_b^- & \frac{\Xi_b^-}{\sqrt{2}} \\ \frac{\Xi_b^0}{\sqrt{2}} & \frac{\Xi_b^-}{\sqrt{2}} & \Omega_b^- \end{pmatrix}, \\ B_3 \left(J^P = \frac{1}{2}^+ \right) = & \begin{pmatrix} 0 & \Lambda_b^0 & \Xi_b^0 \\ -\Lambda_b^0 & 0 & \Xi_b^- \\ -\Xi_b^0 & -\Xi_b^- & 0 \end{pmatrix}. \end{aligned} \tag{A11}$$

Strong coupling constants are collected in Tables 6, 7 and 8.

Appendix B: Expressions of amplitudes

The expressions of amplitudes for all the $B_{bc} \rightarrow B_b P$ decays are collected in this Appendix.

$$\begin{aligned} \mathcal{A}(\Xi_{bc}^+ \rightarrow \Lambda_b^0 K^+) = & \mathcal{T}(\Xi_{bc}^+ \rightarrow \Lambda_b^0 K^+) + \mathcal{M}(K^+, \Lambda_b^0; \omega) + \mathcal{M}(K^+, \Sigma_b^0; \rho^0) \\ & + \mathcal{M}(K^{*+}, \Lambda_b^0; \eta_8) + \mathcal{M}(K^{*+}, \Sigma_b^0; \pi^0) \\ & + \mathcal{M}(K^+, \Lambda_b^0; \Xi_b^-) + \mathcal{M}(K^+, \Lambda_b^0; \Xi_b'^-) + \mathcal{M}(K^+, \Sigma_b^0; \Xi_b^-) \\ & + \mathcal{M}(K^+, \Sigma_b^0; \Xi_b'^-) + \mathcal{M}(K^{*+}, \Lambda_b^0; \Xi_b^-) \\ & + \mathcal{M}(K^{*+}, \Lambda_b^0; \Xi_b'^-) + \mathcal{M}(K^{*+}, \Sigma_b^0; \Xi_b^-) \\ & + \mathcal{M}(K^{*+}, \Sigma_b^0; \Xi_b'^-), \end{aligned} \tag{B1}$$

$$\begin{aligned} \mathcal{A}(\Xi_{bc}^+ \rightarrow \Lambda_b^0 \pi^+) = & \mathcal{T}(\Xi_{bc}^+ \rightarrow \Lambda_b^0 \pi^+) + \mathcal{M}(\pi^+, \Sigma_b^0; \rho^0) + \mathcal{M}(\rho^+, \Sigma_b^0; \pi^0) \\ & + \mathcal{M}(K^+, \Xi_b^0; K^{*0}) + \mathcal{M}(K^+, \Xi_b^0; K^0) \\ & + \mathcal{M}(K^{*+}, \Xi_b^0; K^0) + \mathcal{M}(K^{*+}, \Xi_b^0; K^{*0}) \\ & + \mathcal{M}(\pi^+, \Lambda_b^0; \Sigma_b^-) + \mathcal{M}(\pi^+, \Sigma_b^0; \Sigma_b^-) + \mathcal{M}(\rho^+, \Lambda_b^0; \Sigma_b^-) \\ & + \mathcal{M}(\rho^+, \Sigma_b^0; \Sigma_b^-) + \mathcal{M}(K^+, \Xi_b^0; \Xi_b^-) + \mathcal{M}(K^+, \Xi_b^0; \Xi_b'^-) \\ & + \mathcal{M}(K^+, \Xi_b^0; \Xi_b^-) + \mathcal{M}(K^+, \Xi_b^0; \Xi_b'^-) \\ & + \mathcal{M}(K^{*+}, \Xi_b^0; \Xi_b^-) + \mathcal{M}(K^{*+}, \Xi_b^0; \Xi_b'^-) \\ & + \mathcal{M}(K^{*+}, \Xi_b^0; \Xi_b^-) + \mathcal{M}(K^{*+}, \Xi_b^0; \Xi_b'^-), \end{aligned} \tag{B2}$$

$$\begin{aligned} \mathcal{A}(\Xi_{bc}^+ \rightarrow \Xi_b^0 K^+) = & \mathcal{T}(\Xi_{bc}^+ \rightarrow \Xi_b^0 K^+) + \mathcal{M}(K^+, \Xi_b^0; \rho^0) + \mathcal{M}(K^+, \Xi_b^0; \omega) \\ & + \mathcal{M}(K^+, \Xi_b^0; \rho^0) + \mathcal{M}(K^+, \Xi_b^0; \omega) \\ & + \mathcal{M}(K^{*+}, \Xi_b^0; \pi^0) + \mathcal{M}(K^{*+}, \Xi_b^0; \eta_8) + \mathcal{M}(K^{*+}, \Xi_b^0; \pi^0) \\ & + \mathcal{M}(K^{*+}, \Xi_b^0; \eta_8) + \mathcal{M}(\pi^+, \Lambda_b^0; \bar{K}^{*0}) \\ & + \mathcal{M}(\pi^+, \Sigma_b^0; \bar{K}^{*0}) + \mathcal{M}(\rho^+, \Lambda_b^0; \bar{K}^0) \\ & + \mathcal{M}(\rho^+, \Sigma_b^0; \bar{K}^0) + \mathcal{M}(K^+, \Xi_b^0; \phi) + \mathcal{M}(K^+, \Xi_b^0; \phi) \\ & + \mathcal{M}(K^{*+}, \Xi_b^0; \eta_8) + \mathcal{M}(K^{*+}, \Xi_b^0; \eta_8) \\ & + \mathcal{M}(K^+, \Xi_b^0; \Omega_b^-) + \mathcal{M}(K^+, \Xi_b^0; \Omega_b^-) + \mathcal{M}(K^{*+}, \Xi_b^0; \Omega_b^-) \\ & + \mathcal{M}(K^{*+}, \Xi_b^0; \Omega_b^-) + \mathcal{M}(\pi^+, \Lambda_b^0; \Xi_b^-) + \mathcal{M}(\pi^+, \Lambda_b^0; \Xi_b'^-) \\ & + \mathcal{M}(\pi^+, \Sigma_b^0; \Xi_b^-) + \mathcal{M}(\pi^+, \Sigma_b^0; \Xi_b'^-) \\ & + \mathcal{M}(\rho^+, \Lambda_b^0; \Xi_b^-) + \mathcal{M}(\rho^+, \Lambda_b^0; \Xi_b'^-) \\ & + \mathcal{M}(\rho^+, \Sigma_b^0; \Xi_b^-) + \mathcal{M}(\rho^+, \Sigma_b^0; \Xi_b'^-), \end{aligned} \tag{B3}$$

$$\begin{aligned} \mathcal{A}(\Xi_{bc}^+ \rightarrow \Xi_b^0 \pi^+) = & \mathcal{T}(\Xi_{bc}^+ \rightarrow \Xi_b^0 \pi^+) + \mathcal{M}(\pi^+, \Xi_b^0; \rho^0) \\ & + \mathcal{M}(\pi^+, \Xi_b^0; \rho^0) + \mathcal{M}(\rho^+, \Xi_b^0; \pi^0) + \mathcal{M}(\rho^+, \Xi_b^0; \pi^0) \\ & + \mathcal{M}(\pi^+, \Xi_b^0; \Xi_b^-) + \mathcal{M}(\pi^+, \Xi_b^0; \Xi_b'^-) + \mathcal{M}(\pi^+, \Xi_b^0; \Xi_b^-) \\ & + \mathcal{M}(\pi^+, \Xi_b^0; \Xi_b'^-) + \mathcal{M}(\rho^+, \Xi_b^0; \Xi_b^-) \\ & + \mathcal{M}(\rho^+, \Xi_b^0; \Xi_b'^-) + \mathcal{M}(\rho^+, \Xi_b^0; \Xi_b^-) \\ & + \mathcal{M}(\rho^+, \Xi_b^0; \Xi_b'^-), \end{aligned} \tag{B4}$$

$$\mathcal{A}(\Xi_{bc}^0 \rightarrow \Lambda_b^0 \eta_8) = C_{SD}(\Xi_{bc}^0 \rightarrow \Lambda_b^0 \eta_8) + \mathcal{M}(K^+, \Xi_b^-; K^{*+})$$

Table 6 Strong coupling constants of VPP and VVV vertices

Vertex	g	Vertex	g	Vertex	g	Vertex	g	Vertex	g
$\rho^+ \rightarrow \pi^0 \pi^+$	6.05	$\rho^0 \rightarrow \pi^+ \pi^-$	6.05	$\rho^+ \rightarrow K^+ \bar{K}^0$	4.60	$\rho^0 \rightarrow K^0 \bar{K}^0$	-3.25	$\rho^0 \rightarrow K^+ K^-$	3.25
$\phi \rightarrow K^- K^+$	4.60	$\bar{K}^{*0} \rightarrow \eta_8 \bar{K}^0$	5.63	$\bar{K}^{*0} \rightarrow K^- \pi^+$	4.60	$\bar{K}^{*0} \rightarrow \bar{K}^0 \pi^0$	-3.25	$K^{*+} \rightarrow K^+ \pi^0$	3.25
$K^{*+} \rightarrow \eta_8 K^+$	5.63	$K^{*+} \rightarrow \pi^+ K^0$	4.60	$K^{*0} \rightarrow \pi^- K^+$	4.60	$K^{*0} \rightarrow K^0 \eta_8$	5.63	$K^{*0} \rightarrow \pi^0 K^0$	-3.25
$\omega \rightarrow K^+ K^-$	3.25	$\phi \rightarrow \bar{K}^0 K^0$	4.60	$\omega \rightarrow K^0 \bar{K}^0$	3.25				
$\rho^+ \rightarrow \rho^0 \rho^+$	7.38	$\rho^0 \rightarrow \rho^- \rho^+$	7.38	$\rho^+ \rightarrow K^{*+} \bar{K}^{*0}$	5.22	$\rho^0 \rightarrow K^{*+} K^{*-}$	3.69	$\omega \rightarrow K^{*+} K^{*-}$	3.69
$\bar{K}^{*0} \rightarrow \phi \bar{K}^{*0}$	5.22	$\bar{K}^{*0} \rightarrow \bar{K}^{*0} \rho^0$	-3.69	$\bar{K}^{*0} \rightarrow \bar{K}^{*0} \omega$	3.69	$K^{*+} \rightarrow \rho^+ K^{*0}$	5.22	$K^{*+} \rightarrow \phi K^{*+}$	5.22
$K^{*+} \rightarrow \omega K^{*+}$	3.69	$K^{*0} \rightarrow \rho^0 K^{*0}$	-3.69	$K^{*0} \rightarrow \omega K^{*0}$	3.69	$K^{*0} \rightarrow K^{*0} \phi$	5.22	$\phi \rightarrow K^{*-} K^{*+}$	5.22
$\omega \rightarrow K^{*0} \bar{K}^{*0}$	3.69	$\phi \rightarrow \bar{K}^{*0} K^{*0}$	5.22	$\rho^0 \rightarrow K^{*0} \bar{K}^{*0}$	-3.69	$K^{*+} \rightarrow K^{*+} \rho^0$	3.69	$\bar{K}^{*0} \rightarrow K^{*-} \rho^+$	5.22

Table 7 Strong coupling constants of PB_3B_3 , PB_3B_6 and PB_6B_6 vertex

Vertex	g	Vertex	g	Vertex	g	Vertex	g	Vertex	g
$\Xi_b^0 \rightarrow \Lambda_b^0 \bar{K}^0$	1.5	$\Lambda_b^0 \rightarrow \Xi_b^0 K^0$	1.5	$\Xi_b^0 \rightarrow \Xi_b^0 \eta_8$	-0.5	$\Lambda_b^0 \rightarrow \Lambda_b^0 \eta_8$	1.0	$\Xi_b^- \rightarrow \Lambda_b^0 K^-$	-1.5
$\Xi_b^- \rightarrow \Xi_b^- \eta_8$	-0.41	$\Xi_b^- \rightarrow \Xi_b^0 \pi^-$	1.0	$\Xi_b^0 \rightarrow \Xi_b^- \pi^+$	1.0	$\Xi_b^- \rightarrow \Xi_b^- \pi^0$	-0.71	$\Xi_b^0 \rightarrow \Xi_b^0 \pi^0$	1.0
$\Sigma_b^0 \rightarrow \Xi_b^0 K^0$	-11.5	$\Xi_b^0 \rightarrow \Sigma_b^+ K^-$	-17.0	$\Sigma_b^+ \rightarrow \Xi_b^0 K^+$	-17.0	$\Xi_b^0 \rightarrow \Xi_b^0 \eta_8$	16.0	$\Xi_b^0 \rightarrow \Xi_b^0 \eta_8$	16.0
$\Sigma_b^0 \rightarrow \Lambda_b^0 \pi^0$	18.5	$\Lambda_b^0 \rightarrow \Sigma_b^+ \pi^-$	-15.0	$\Sigma_b^+ \rightarrow \Lambda_b^0 \pi^+$	-15.0	$\Lambda_b^0 \rightarrow \Sigma_b^- \pi^+$	15.0	$\Sigma_b^- \rightarrow \Lambda_b^0 \pi^-$	15.0
$\Xi_b^0 \rightarrow \Lambda_b^0 \bar{K}^0$	-11.5	$\Lambda_b^0 \rightarrow \Xi_b^- K^+$	11.5	$\Xi_b^- \rightarrow \Lambda_b^0 K^-$	11.5	$\Xi_b^- \rightarrow \Sigma_b^0 K^-$	-11.5	$\Sigma_b^0 \rightarrow \Xi_b^- K^+$	-11.5
$\Sigma_b^- \rightarrow \Xi_b^- K^0$	-17.0	$\Xi_b^- \rightarrow \Xi_b^- \eta_8$	16.0	$\Xi_b^- \rightarrow \Xi_b^- \eta_8$	16.0	$\Xi_b^- \rightarrow \Omega_b^- K^0$	17.0	$\Omega_b^- \rightarrow \Xi_b^- \bar{K}^0$	17.0
$\Xi_b^0 \rightarrow \Xi_b^- \pi^+$	10.6	$\Xi_b^- \rightarrow \Xi_b^- \pi^0$	-7.5	$\Xi_b^- \rightarrow \Xi_b^- \pi^0$	-7.5	$\Xi_b^0 \rightarrow \Omega_b^- K^+$	17.0	$\Omega_b^- \rightarrow \Xi_b^0 K^-$	17.0
$\Xi_b^0 \rightarrow \Xi_b^0 \pi^0$	7.5	$\Xi_b^0 \rightarrow \Xi_b^- \pi^+$	10.6	$\Xi_b^- \rightarrow \Xi_b^0 \pi^-$	10.6	$\Xi_b^0 \rightarrow \Sigma_b^0 \bar{K}^0$	13.4	$\Sigma_b^0 \rightarrow \Xi_b^0 K^0$	13.4
$\Sigma_b^+ \rightarrow \Xi_b^0 K^+$	19.0	$\Xi_b^0 \rightarrow \Xi_b^0 \eta_8$	-5.3	$\Sigma_b^0 \rightarrow \Sigma_b^0 \eta_8$	12.5	$\Sigma_b^0 \rightarrow \Sigma_b^+ \pi^-$	17.0	$\Sigma_b^+ \rightarrow \Sigma_b^0 \pi^+$	17.0
$\Sigma_b^+ \rightarrow \Sigma_b^+ \pi^0$	18.0	$\Xi_b^- \rightarrow \Sigma_b^0 K^-$	13.4	$\Sigma_b^0 \rightarrow \Xi_b^- K^+$	13.4	$\Xi_b^- \rightarrow \Sigma_b^- \bar{K}^0$	19.0	$\Sigma_b^- \rightarrow \Xi_b^- K^0$	19.0
$\Omega_b^- \rightarrow \Omega_b^- \eta_8$	-26.0	$\Omega_b^- \rightarrow \Xi_b^0 K^-$	21.0	$\Xi_b^0 \rightarrow \Omega_b^- K^+$	21.0	$\Omega_b^- \rightarrow \Xi_b^- \bar{K}^0$	19.0	$\Xi_b^- \rightarrow \Omega_b^- K^0$	19.0
$\Sigma_b^0 \rightarrow \Sigma_b^- \pi^+$	17.0	$\Sigma_b^- \rightarrow \Sigma_b^- \eta_8$	12.5	$\Sigma_b^- \rightarrow \Sigma_b^- \pi^0$	-18.0	$\Xi_b^- \rightarrow \Xi_b^0 \pi^-$	12.0	$\Xi_b^0 \rightarrow \Xi_b^- \pi^+$	12.0
$\Xi_b^0 \rightarrow \Xi_b^0 \pi^0$	9.0	$\Lambda_b^0 \rightarrow \Xi_b^- K^+$	-1.5	$\Xi_b^0 \rightarrow \Sigma_b^0 \bar{K}^0$	-11.5	$\Lambda_b^0 \rightarrow \Sigma_b^0 \pi^0$	18.5	$\Lambda_b^0 \rightarrow \Xi_b^0 K^0$	-11.5
$\Xi_b^- \rightarrow \Sigma_b^- \bar{K}^0$	-17.0	$\Xi_b^- \rightarrow \Xi_b^0 \pi^-$	10.6	$\Xi_b^0 \rightarrow \Xi_b^0 \pi^0$	7.5	$\Xi_b^0 \rightarrow \Sigma_b^+ K^-$	19.0	$\Sigma_b^+ \rightarrow \Sigma_b^+ \eta_8$	12.5
$\Xi_b^- \rightarrow \Xi_b^- \eta_8$	-5.5	$\Sigma_b^- \rightarrow \Sigma_b^0 \pi^-$	17.0	$\Xi_b^- \rightarrow \Xi_b^- \pi^0$	-9.0				

$$\begin{aligned}
 & + \mathcal{M}(K^+, \Xi_b^-; K^{*+}) + \mathcal{M}(K^{*+}, \Xi_b^-; K^+) \\
 & + \mathcal{M}(K^{*+}, \Xi_b^-; K^+) + \mathcal{M}(K^+, \Xi_b^-; \Xi_b^-) \\
 & + \mathcal{M}(K^+, \Xi_b^-; \Xi_b^-) + \mathcal{M}(K^+, \Xi_b^-; \Xi_b^-) \\
 & + \mathcal{M}(K^+, \Xi_b^-; \Xi_b^-) + \mathcal{M}(K^{*+}, \Xi_b^-; \Xi_b^-) \\
 & + \mathcal{M}(K^{*+}, \Xi_b^-; \Xi_b^-) + \mathcal{M}(K^{*+}, \Xi_b^-; \Xi_b^-) \\
 & + \mathcal{M}(K^{*+}, \Xi_b^-; \Xi_b^-) + \mathcal{M}(\pi^+, \Sigma_b^-; \Sigma_b^-) \\
 & + \mathcal{M}(\rho^+, \Sigma_b^-; \Sigma_b^-),
 \end{aligned}$$

(B5)

$$\begin{aligned}
 \mathcal{A}(\Xi_{bc}^0 \rightarrow \Lambda_b^0 \bar{K}^0) &= C_{SD}(\Xi_{bc}^0 \rightarrow \Lambda_b^0 \bar{K}^0) + \mathcal{M}(\pi^+, \Xi_b^-; K^{*+}) \\
 & + \mathcal{M}(\pi^+, \Xi_b^-; K^{*+}) \\
 & + \mathcal{M}(\rho^+, \Xi_b^-; K^+) + \mathcal{M}(\rho^+, \Xi_b^-; K^+) \\
 & + \mathcal{M}(\pi^+, \Xi_b^-; \Sigma_b^-) + \mathcal{M}(\pi^+, \Xi_b^-; \Sigma_b^-) \\
 & + \mathcal{M}(\rho^+, \Xi_b^-; \Sigma_b^-) + \mathcal{M}(\rho^+, \Xi_b^-; \Sigma_b^-),
 \end{aligned}$$

(B6)

$$\begin{aligned}
 \mathcal{A}(\Xi_{bc}^0 \rightarrow \Lambda_b^0 K^0) &= C_{SD}(\Xi_{bc}^0 \rightarrow \Lambda_b^0 K^0) + \mathcal{M}(K^+, \Sigma_b^-; \rho^+) \\
 & + \mathcal{M}(K^{*+}, \Sigma_b^-; \pi^+) + \mathcal{M}(K^+, \Sigma_b^-; \Xi_b^-) \\
 & + \mathcal{M}(K^+, \Sigma_b^-; \Xi_b^-) + \mathcal{M}(K^{*+}, \Sigma_b^-; \Xi_b^-) \\
 & + \mathcal{M}(K^{*+}, \Sigma_b^-; \Xi_b^-),
 \end{aligned}$$

(B7)

$$\begin{aligned}
 \mathcal{A}(\Xi_{bc}^0 \rightarrow \Lambda_b^0 \pi^0) &= C_{SD}(\Xi_{bc}^0 \rightarrow \Lambda_b^0 \pi^0) + \mathcal{M}(\pi^+, \Sigma_b^-; \rho^+) \\
 & + \mathcal{M}(\rho^+, \Sigma_b^-; \pi^+) + \mathcal{M}(K^+, \Xi_b^-; K^{*+}) \\
 & + \mathcal{M}(K^+, \Xi_b^-; K^{*+}) + \mathcal{M}(K^{*+}, \Xi_b^-; K^+) \\
 & + \mathcal{M}(K^{*+}, \Xi_b^-; K^+) + \mathcal{M}(\pi^+, \Sigma_b^-; \Sigma_b^-) \\
 & + \mathcal{M}(\rho^+, \Sigma_b^-; \Sigma_b^-) + \mathcal{M}(K^+, \Xi_b^-; \Xi_b^-) \\
 & + \mathcal{M}(K^+, \Xi_b^-; \Xi_b^-) + \mathcal{M}(K^+, \Xi_b^-; \Xi_b^-) \\
 & + \mathcal{M}(K^+, \Xi_b^-; \Xi_b^-)
 \end{aligned}$$

(B8)

$$\begin{aligned}
 \mathcal{A}(\Xi_{bc}^0 \rightarrow \Xi_b^- K^+) &= \mathcal{T}(\Xi_{bc}^0 \rightarrow \Xi_b^- K^+) + \mathcal{M}(\pi^+, \Sigma_b^-; \bar{K}^{*0}) + \mathcal{M}(\rho^+, \Sigma_b^-; \bar{K}^0) \\
 & + \mathcal{M}(K^+, \Xi_b^-; \phi) + \mathcal{M}(K^+, \Xi_b^-; \phi) \\
 & + \mathcal{M}(K^{*+}, \Xi_b^-; \eta_8) \\
 & + \mathcal{M}(K^{*+}, \Xi_b^-; \eta_8),
 \end{aligned}$$

(B9)

$$\begin{aligned}
 \mathcal{A}(\Xi_{bc}^0 \rightarrow \Xi_b^- \pi^+) &= \mathcal{T}(\Xi_{bc}^0 \rightarrow \Xi_b^- \pi^+) + \mathcal{M}(\pi^+, \Xi_b^-; \rho^0) + \mathcal{M}(\pi^+, \Xi_b^-; \rho^0) \\
 & + \mathcal{M}(\rho^+, \Xi_b^-; \pi^0) + \mathcal{M}(\rho^+, \Xi_b^-; \pi^0)
 \end{aligned}$$

(B10)

$$\begin{aligned}
 \mathcal{A}(\Xi_{bc}^0 \rightarrow \Xi_b^0 \eta_8) &= \mathcal{M}(\pi^+, \Xi_b^-; \Xi_b^-) + \mathcal{M}(\pi^+, \Xi_b^-; \Xi_b^-) \\
 & + \mathcal{M}(\pi^+, \Xi_b^-; \Xi_b^-) + \mathcal{M}(\pi^+, \Xi_b^-; \Xi_b^-) + \mathcal{M}(\rho^+, \Xi_b^-; \Xi_b^-) \\
 & + \mathcal{M}(\rho^+, \Xi_b^-; \Xi_b^-) + \mathcal{M}(\rho^+, \Xi_b^-; \Xi_b^-)
 \end{aligned}$$

Table 8 Strong coupling constants of $V\mathcal{B}_3\mathcal{B}_3$, $V\mathcal{B}_3\mathcal{B}_6$ and $V\mathcal{B}_6\mathcal{B}_6$ vertex

Vertex	f_1	f_2	Vertex	f_1	f_2	Vertex	f_1	f_2	Vertex	f_1	f_2
$\Lambda_b^0 \rightarrow \Lambda_b^0 \omega$	5.2	8.0	$\Lambda_b^0 \rightarrow \Xi_b^0 K^{*0}$	5.0	7.0	$\Xi_b^0 \rightarrow \Lambda_b^0 \bar{K}^{*0}$	5.0	7.0	$\Xi_b^0 \rightarrow \Xi_b^0 \phi$	4.0	5.7
$\Xi_b^- \rightarrow \Lambda_b^0 K^{*-}$	-5.0	-7.0	$\Xi_b^- \rightarrow \Xi_b^- \phi$	4.0	5.7	$\Xi_b^- \rightarrow \Xi_b^0 \rho^-$	4.4	7.1	$\Xi_b^0 \rightarrow \Xi_b^- \rho^+$	4.4	7.1
$\Xi_b^- \rightarrow \Xi_b^- \rho^0$	-3.1	-5.0	$\Xi_b^0 \rightarrow \Xi_b^0 \omega$	2.8	4.0	$\Xi_b^0 \rightarrow \Xi_b^0 \rho^0$	3.1	5.0	$\Lambda_b^0 \rightarrow \Sigma_b^0 \rho^0$	2.8	40.0
$\Lambda_b^0 \rightarrow \Sigma_b^+ \rho^-$	-2.8	-40.0	$\Sigma_b^+ \rightarrow \Lambda_b^0 \rho^+$	-2.8	-40.0	$\Lambda_b^0 \rightarrow \Xi_b^0 K^{*0}$	-2.6	-32.0	$\Xi_b^0 \rightarrow \Lambda_b^0 \bar{K}^{*0}$	-2.6	-32.0
$\Sigma_b^0 \rightarrow \Xi_b^0 K^{*0}$	-2.6	-32.0	$\Xi_b^0 \rightarrow \Sigma_b^+ K^{*-}$	-3.7	-45.3	$\Sigma_b^+ \rightarrow \Xi_b^0 K^{*+}$	-3.7	-45.3	$\Xi_b^0 \rightarrow \Xi_b^0 \phi$	-2.6	-30.0
$\Lambda_b^0 \rightarrow \Sigma_b^- \rho^+$	2.8	40.0	$\Sigma_b^- \rightarrow \Lambda_b^0 \rho^-$	2.8	40.0	$\Lambda_b^0 \rightarrow \Xi_b'^- K^{*+}$	2.6	32.0	$\Xi_b'^- \rightarrow \Lambda_b^0 K^{*-}$	2.6	32.0
$\Sigma_b^0 \rightarrow \Xi_b^- K^{*+}$	-2.6	-32.0	$\Xi_b^- \rightarrow \Sigma_b^- K^{*0}$	-3.7	-45.3	$\Sigma_b^- \rightarrow \Xi_b^- K^{*0}$	-3.7	-45.3	$\Xi_b^- \rightarrow \Xi_b'^- \phi$	-2.6	-30.0
$\Xi_b^- \rightarrow \Omega_b^- K^{*0}$	3.5	50.0	$\Omega_b^- \rightarrow \Xi_b^- K^{*0}$	3.5	50.0	$\Xi_b^- \rightarrow \Xi_b^0 \rho^-$	2.0	28.3	$\Xi_b^0 \rightarrow \Xi_b^- \rho^+$	2.0	28.3
$\Xi_b'^- \rightarrow \Xi_b^- \omega$	1.4	22.0	$\Xi_b^- \rightarrow \Xi_b'^- \rho^0$	-1.4	-20.0	$\Xi_b'^- \rightarrow \Xi_b^- \rho^0$	-1.4	-20.0	$\Xi_b^0 \rightarrow \Omega_b^- K^{*+}$	3.7	45.3
$\Xi_b^0 \rightarrow \Xi_b'^- \rho^+$	2.0	28.3	$\Xi_b'^- \rightarrow \Xi_b^0 \rho^-$	2.0	28.3	$\Xi_b^0 \rightarrow \Xi_b^0 \omega$	1.4	22.0	$\Xi_b^0 \rightarrow \Xi_b^0 \omega$	1.4	22.0
$\Xi_b^0 \rightarrow \Xi_b^0 \rho^0$	1.4	22.0	$\Sigma_b^0 \rightarrow \Sigma_b^0 \omega$	4.0	50.0	$\Sigma_b^0 \rightarrow \Sigma_b^+ \rho^-$	4.5	55.0	$\Sigma_b^+ \rightarrow \Sigma_b^0 \rho^+$	4.5	55.0
$\Xi_b^0 \rightarrow \Sigma_b^0 \bar{K}^{*0}$	4.2	42.4	$\Sigma_b^+ \rightarrow \Sigma_b^+ \omega$	4.0	50.0	$\Sigma_b^+ \rightarrow \Sigma_b^+ \rho^0$	4.4	60.0	$\Sigma_b^+ \rightarrow \Xi_b^0 K^{*+}$	6.0	60.0
$\Xi_b^0 \rightarrow \Xi_b^0 \phi$	5.0	45.0	$\Omega_b^- \rightarrow \Omega_b^- \phi$	10.0	95.0	$\Omega_b^- \rightarrow \Xi_b^0 K^{*-}$	6.0	70.0	$\Xi_b^0 \rightarrow \Omega_b^- K^{*+}$	6.0	70.0
$\Xi_b'^- \rightarrow \Omega_b^- K^{*0}$	6.0	60.0	$\Sigma_b^- \rightarrow \Sigma_b^0 \rho^-$	4.5	55.0	$\Sigma_b^0 \rightarrow \Sigma_b^- \rho^+$	4.5	55.0	$\Sigma_b^- \rightarrow \Sigma_b^- \omega$	4.0	50.0
$\Sigma_b^- \rightarrow \Xi_b^- K^{*0}$	6.0	60.0	$\Xi_b^- \rightarrow \Sigma_b^- K^{*0}$	6.0	60.0	$\Sigma_b^0 \rightarrow \Xi_b'^- K^{*+}$	4.2	42.4	$\Xi_b'^- \rightarrow \Sigma_b^0 K^{*-}$	4.2	42.4
$\Xi_b^- \Xi_b^0 \rho^-$	3.2	38.9	$\Xi_b^0 \rightarrow \Xi_b'^- \rho^+$	3.2	38.9	$\Xi_b'^- \rightarrow \Xi_b^- \omega$	2.0	25.0	$\Xi_b'^- \rightarrow \Xi_b^- \rho^0$	-2.2	-30.0
$\Xi_b^0 \rightarrow \Xi_b^0 \rho^0$	2.2	30.0	$\Lambda_b^0 \rightarrow \Xi_b^- K^{*+}$	-5.0	-7.0	$\Xi_b^- \rightarrow \Xi_b^- \omega$	2.8	4.0	$\Sigma_b^0 \rightarrow \Lambda_b^0 \rho^0$	2.8	40.0
$\Xi_b^0 \rightarrow \Sigma_b^0 \bar{K}^{*0}$	-2.6	-32.0	$\Xi_b^0 \rightarrow \Xi_b^0 \phi$	-2.6	-30.0	$\Xi_b^- \rightarrow \Sigma_b^0 K^{*-}$	-2.6	-32.0	$\Xi_b^- \rightarrow \Xi_b^- \phi$	-2.6	-30.0
$\Xi_b^- \rightarrow \Xi_b^- \omega$	1.4	22.0	$\Omega_b^- \rightarrow \Xi_b^0 K^{*-}$	3.7	45.3	$\Xi_b^0 \rightarrow \Xi_b^0 \rho^0$	1.4	22.0	$\Sigma_b^0 \rightarrow \Xi_b^0 K^{*0}$	4.2	42.4
$\Xi_b^0 \rightarrow \Sigma_b^+ K^{*-}$	6.0	60.0	$\Omega_b^- \rightarrow \Xi_b^- K^{*0}$	6.0	60.0	$\Sigma_b^- \rightarrow \Sigma_b^- \rho^0$	-4.4	-60.0	$\Xi_b'^- \rightarrow \Xi_b^- \phi$	5.0	45.0
$\Xi_b^0 \rightarrow \Xi_b^0 \omega$	2.1	27.0									

$$+ \mathcal{M}(\rho^+, \Xi_b'^-; \Xi_b^-) \tag{B11}$$

$$\begin{aligned} \mathcal{A}(\Xi_b^0 \rightarrow \Xi_b^0 K^0) = & C_{SD}(\Xi_b^0 \rightarrow \Xi_b^0 K^0) + \mathcal{M}(K^+, \Xi_b^-; \rho^+) + \mathcal{M}(K^+, \Xi_b'^-; \rho^+) \\ & + \mathcal{M}(K^{*+}, \Xi_b^-; \pi^+) + \mathcal{M}(K^{*+}, \Xi_b'^-; \pi^+) \\ & + \mathcal{M}(K^+, \Xi_b^-; \Omega_b^-) + \mathcal{M}(K^+, \Xi_b'^-; \Omega_b^-) + \mathcal{M}(K^{*+}, \Xi_b^-; \Omega_b^-) \\ & + \mathcal{M}(K^{*+}, \Xi_b'^-; \Omega_b^-) + \mathcal{M}(\pi^+, \Sigma_b^-; \Xi_b^-) \\ & + \mathcal{M}(\pi^+, \Sigma_b^-; \Xi_b'^-) + \mathcal{M}(\rho^+, \Sigma_b^-; \Xi_b^-) \\ & + \mathcal{M}(\rho^+, \Sigma_b^-; \Xi_b'^-), \end{aligned} \tag{B12}$$

$$\begin{aligned} \mathcal{A}(\Xi_b^0 \rightarrow \Xi_b^0 \pi^0) = & C_{SD}(\Xi_b^0 \rightarrow \Xi_b^0 \pi^0) + \mathcal{M}(\pi^+, \Xi_b^-; \rho^+) + \mathcal{M}(\pi^+, \Xi_b'^-; \rho^+) \\ & + \mathcal{M}(\rho^+, \Xi_b^-; \pi^+) + \mathcal{M}(\rho^+, \Xi_b'^-; \pi^+) \\ & + \mathcal{M}(\pi^+, \Xi_b^-; \Xi_b^-) + \mathcal{M}(\pi^+, \Xi_b^-; \Xi_b'^-) + \mathcal{M}(\pi^+, \Xi_b'^-; \Xi_b^-) \\ & + \mathcal{M}(\pi^+, \Xi_b'^-; \Xi_b^-) + \mathcal{M}(\rho^+, \Xi_b^-; \Xi_b^-) \\ & + \mathcal{M}(\rho^+, \Xi_b^-; \Xi_b'^-) + \mathcal{M}(\rho^+, \Xi_b'^-; \Xi_b^-) \\ & + \mathcal{M}(\rho^+, \Xi_b'^-; \Xi_b'^-), \end{aligned} \tag{B13}$$

$$\mathcal{A}(\Xi_b^0 \rightarrow \Sigma_b^- K^+) = \mathcal{T}(\Xi_b^0 \rightarrow \Sigma_b^- K^+), \tag{B14}$$

$$\mathcal{A}(\Omega_b^0 \rightarrow \Omega_b^- \pi^+) = \mathcal{T}(\Omega_b^0 \rightarrow \Omega_b^- \pi^+), \tag{B15}$$

$$\begin{aligned} \mathcal{A}(\Omega_b^0 \rightarrow \Lambda_b^0 \eta_8) = & C_{SD}(\Omega_b^0 \rightarrow \Lambda_b^0 \eta_8) + \mathcal{M}(K^+, \Xi_b^-; K^{*+}) \\ & + \mathcal{M}(K^+, \Xi_b'^-; K^{*+}) + \mathcal{M}(K^{*+}, \Xi_b^-; K^+) + \mathcal{M}(K^{*+}, \Xi_b'^-; K^+) \\ & + \mathcal{M}(K^+, \Xi_b^-; \Xi_b^-) + \mathcal{M}(K^+, \Xi_b^-; \Xi_b'^-) + \mathcal{M}(K^+, \Xi_b'^-; \Xi_b^-) \\ & + \mathcal{M}(K^+, \Xi_b'^-; \Xi_b^-) + \mathcal{M}(K^{*+}, \Xi_b^-; \Xi_b^-) \\ & + \mathcal{M}(K^{*+}, \Xi_b'^-; \Xi_b^-) + \mathcal{M}(K^{*+}, \Omega_b^-; \bar{K}^0) \\ & + \mathcal{M}(K^{*+}, \Omega_b^-; \bar{K}^0), \end{aligned} \tag{B16}$$

$$\begin{aligned} \mathcal{A}(\Omega_b^0 \rightarrow \Lambda_b^0 \bar{K}^0) = & C_{SD}(\Omega_b^0 \rightarrow \Lambda_b^0 \bar{K}^0) + \mathcal{M}(\pi^+, \Xi_b^-; K^{*+}) \\ & + \mathcal{M}(\pi^+, \Xi_b'^-; K^{*+}) + \mathcal{M}(\rho^+, \Xi_b^-; K^+) + \mathcal{M}(\rho^+, \Xi_b'^-; K^+) \end{aligned}$$

$$\begin{aligned} & + \mathcal{M}(\pi^+, \Xi_b^-; \Sigma_b^-) + \mathcal{M}(\pi^+, \Xi_b'^-; \Sigma_b^-) \\ & + \mathcal{M}(\rho^+, \Xi_b^-; \Sigma_b^-) + \mathcal{M}(\rho^+, \Xi_b'^-; \Sigma_b^-) + \mathcal{M}(K^+, \Omega_b^-; \Xi_b^-) \\ & + \mathcal{M}(K^+, \Omega_b^-; \Xi_b'^-) + \mathcal{M}(K^{*+}, \Omega_b^-; \Xi_b^-) \\ & + \mathcal{M}(K^{*+}, \Omega_b^-; \Xi_b'^-), \end{aligned} \tag{B17}$$

$$\begin{aligned} \mathcal{A}(\Omega_b^0 \rightarrow \Lambda_b^0 \pi^0) = & \mathcal{M}(K^+, \Xi_b^-; K^{*+}) + \mathcal{M}(K^+, \Xi_b'^-; K^{*+}) \\ & + \mathcal{M}(K^{*+}, \Xi_b^-; K^+) + \mathcal{M}(K^{*+}, \Xi_b'^-; K^+) \\ & + \mathcal{M}(K^+, \Xi_b^-; \Xi_b^-) + \mathcal{M}(K^+, \Xi_b^-; \Xi_b'^-) + \mathcal{M}(K^+, \Xi_b'^-; \Xi_b^-) \\ & + \mathcal{M}(K^+, \Xi_b'^-; \Xi_b^-) \\ & + \mathcal{M}(K^{*+}, \Xi_b^-; \Xi_b^-) + \mathcal{M}(K^{*+}, \Xi_b'^-; \Xi_b^-) \\ & + \mathcal{M}(K^{*+}, \Xi_b^-; \Xi_b^-) + \mathcal{M}(K^{*+}, \Xi_b'^-; \Xi_b^-), \end{aligned} \tag{B18}$$

$$\begin{aligned} \mathcal{A}(\Omega_b^0 \rightarrow \Xi_b^- K^+) = & \mathcal{T}(\Omega_b^0 \rightarrow \Xi_b^- K^+) + \mathcal{M}(K^+, \Xi_b^-; \phi) + \mathcal{M}(K^+, \Xi_b'^-; \phi) \\ & + \mathcal{M}(K^{*+}, \Xi_b^-; \eta_8) + \mathcal{M}(K^{*+}, \Xi_b'^-; \eta_8), \end{aligned} \tag{B19}$$

$$\begin{aligned} \mathcal{A}(\Omega_b^0 \rightarrow \Xi_b^- \pi^+) = & \mathcal{T}(\Omega_b^0 \rightarrow \Xi_b^- \pi^+) + \mathcal{M}(\pi^+, \Xi_b^-; \rho^0) + \mathcal{M}(\pi^+, \Xi_b'^-; \rho^0) \\ & + \mathcal{M}(\rho^+, \Xi_b^-; \pi^0) + \mathcal{M}(\rho^+, \Xi_b'^-; \pi^0) \\ & + \mathcal{M}(K^+, \Omega_b^-; K^{*0}) + \mathcal{M}(K^{*+}, \Omega_b^-; \bar{K}^0), \end{aligned} \tag{B20}$$

$$\begin{aligned} \mathcal{A}(\Omega_b^0 \rightarrow \Xi_b^0 \eta_8) = & C_{SD}(\Omega_b^0 \rightarrow \Xi_b^0 \eta_8) + \mathcal{M}(K^+, \Omega_b^-; K^{*+}) \\ & + \mathcal{M}(K^{*+}, \Omega_b^-; K^+) + \mathcal{M}(K^+, \Omega_b^-; \Omega_b^-) + \mathcal{M}(K^{*+}, \Omega_b^-; \Omega_b^-) \\ & + \mathcal{M}(\pi^+, \Xi_b^-; \Xi_b^-) + \mathcal{M}(\pi^+, \Xi_b^-; \Xi_b'^-) + \mathcal{M}(\pi^+, \Xi_b'^-; \Xi_b^-) \\ & + \mathcal{M}(\pi^+, \Xi_b'^-; \Xi_b^-) + \mathcal{M}(\rho^+, \Xi_b^-; \Xi_b^-) \\ & + \mathcal{M}(\rho^+, \Xi_b^-; \Xi_b'^-) + \mathcal{M}(\rho^+, \Xi_b'^-; \Xi_b^-) \\ & + \mathcal{M}(\rho^+, \Xi_b'^-; \Xi_b'^-), \end{aligned} \tag{B21}$$

$$\begin{aligned} \mathcal{A}(\Omega_b^0 \rightarrow \Xi_b^0 \bar{K}^0) = & C_{SD}(\Omega_b^0 \rightarrow \Xi_b^0 \bar{K}^0) + \mathcal{M}(\pi^+, \Omega_b^-; K^{*+}) + \mathcal{M}(\rho^+, \Omega_b^-; K^+) \\ & + \mathcal{M}(\pi^+, \Omega_b^-; \Xi_b^-) + \mathcal{M}(\pi^+, \Omega_b^-; \Xi_b'^-) \end{aligned}$$

$$\begin{aligned}
& + \mathcal{M}(\rho^+, \Omega_b^-; \Xi_b^-) \\
& + \mathcal{M}(\rho^+, \Omega_b^-; \Xi_b'^-), \quad (\text{B22})
\end{aligned}$$

$$\begin{aligned}
\mathcal{A}(\Omega_{bc}^0 \rightarrow \Xi_b^0 K^0) &= C_{SD}(\Omega_{bc}^0 \rightarrow \Xi_b^0 K^0) + \mathcal{M}(K^+, \Xi_b^-; \rho^+) + \mathcal{M}(K^+, \Xi_b'^-; \rho^+) \\
& + \mathcal{M}(K^{*+}, \Xi_b^-; \pi^+) + \mathcal{M}(K^{*+}, \Xi_b'^-; \pi^+) \\
& + \mathcal{M}(K^+, \Xi_b^-; \Omega_b^-) + \mathcal{M}(K^+, \Xi_b'^-; \Omega_b^-) \\
& + \mathcal{M}(K^{*+}, \Xi_b^-; \Omega_b^-) + \mathcal{M}(K^{*+}, \Xi_b'^-; \Omega_b^-) \quad (\text{B23})
\end{aligned}$$

$$\begin{aligned}
\mathcal{A}(\Omega_{bc}^0 \rightarrow \Xi_b^0 \pi^0) &= C_{SD}(\Omega_{bc}^0 \rightarrow \Xi_b^0 \pi^0) + \mathcal{M}(\pi^+, \Xi_b^-; \rho^+) + \mathcal{M}(\pi^+, \Xi_b'^-; \rho^+) \\
& + \mathcal{M}(\rho^+, \Xi_b^-; \pi^+) + \mathcal{M}(\rho^+, \Xi_b'^-; \pi^+) \\
& + \mathcal{M}(K^+, \Omega_b^-; K^{*+}) + \mathcal{M}(K^+, \Omega_b^-; K^+) + \mathcal{M}(\pi^+, \Xi_b^-; \Xi_b^-) \\
& + \mathcal{M}(\pi^+, \Xi_b^-; \Xi_b'^-) + \mathcal{M}(\pi^+, \Xi_b'^-; \Xi_b^-) \\
& + \mathcal{M}(\pi^+, \Xi_b'^-; \Xi_b'^-) + \mathcal{M}(\rho^+, \Xi_b^-; \Xi_b^-) \\
& + \mathcal{M}(\rho^+, \Xi_b^-; \Xi_b'^-) + \mathcal{M}(\rho^+, \Xi_b'^-; \Xi_b^-) \\
& + \mathcal{M}(\rho^+, \Xi_b'^-; \Xi_b'^-), \quad (\text{B24})
\end{aligned}$$

$$\begin{aligned}
\mathcal{A}(\Xi_{bc}^+ \rightarrow \Sigma_b^0 K^+) &= \mathcal{T}(\Xi_{bc}^+ \rightarrow \Sigma_b^0 K^+) + \mathcal{M}(K^+, \Lambda_b^0; \rho^0) + \mathcal{M}(K^+, \Sigma_b^0; \omega) \\
& + \mathcal{M}(K^{*+}, \Lambda_b^0; \pi^0) + \mathcal{M}(K^{*+}, \Sigma_b^0; \eta_8) \\
& + \mathcal{M}(K^+, \Lambda_b^0; \Xi_b^-) + \mathcal{M}(K^+, \Lambda_b^0; \Xi_b'^-) \\
& + \mathcal{M}(K^+, \Sigma_b^0; \Xi_b^-) + \mathcal{M}(K^+, \Sigma_b^0; \Xi_b'^-) \\
& + \mathcal{M}(K^{*+}, \Lambda_b^0; \Xi_b^-) \\
& + \mathcal{M}(K^{*+}, \Lambda_b^0; \Xi_b'^-) + \mathcal{M}(K^{*+}, \Sigma_b^0; \Xi_b^-) \\
& + \mathcal{M}(K^{*+}, \Sigma_b^0; \Xi_b'^-), \quad (\text{B25})
\end{aligned}$$

$$\begin{aligned}
\mathcal{A}(\Xi_{bc}^+ \rightarrow \Sigma_b^0 \pi^+) &= \mathcal{T}(\Xi_{bc}^+ \rightarrow \Sigma_b^0 \pi^+) + \mathcal{M}(\pi^+, \Lambda_b^0; \rho^0) \\
& + \mathcal{M}(\rho^+, \Lambda_b^0; \pi^0) + \mathcal{M}(K^+, \Xi_b^0; K^{*0}) \\
& + \mathcal{M}(K^+, \Xi_b^0; K^0) \\
& + \mathcal{M}(K^{*+}, \Xi_b^0; K^0) + \mathcal{M}(\pi^+, \Lambda_b^0; \Sigma_b^-) \\
& + \mathcal{M}(\pi^+, \Sigma_b^0; \Sigma_b^-) + \mathcal{M}(\rho^+, \Lambda_b^0; \Sigma_b^-) \\
& + \mathcal{M}(\rho^+, \Sigma_b^0; \Sigma_b^-) + \mathcal{M}(K^+, \Xi_b^0; \Xi_b^-) \\
& + \mathcal{M}(K^+, \Xi_b^0; \Xi_b'^-) + \mathcal{M}(K^+, \Xi_b^0; \Xi_b'^-) \\
& + \mathcal{M}(K^{*+}, \Xi_b^0; \Xi_b^-) + \mathcal{M}(K^{*+}, \Xi_b^0; \Xi_b'^-) \\
& + \mathcal{M}(K^{*+}, \Xi_b^0; \Xi_b^-) + \mathcal{M}(K^{*+}, \Xi_b^0; \Xi_b'^-), \quad (\text{B26})
\end{aligned}$$

$$\begin{aligned}
\mathcal{A}(\Xi_{bc}^+ \rightarrow \Sigma_b^+ \eta_8) &= C_{SD}(\Xi_{bc}^+ \rightarrow \Sigma_b^+ \eta_8) + \mathcal{M}(\pi^+, \Sigma_b^0; \Sigma_b^0) + \mathcal{M}(\pi^+, \Lambda_b^0; \Lambda_b^0) \\
& + \mathcal{M}(\rho^+, \Sigma_b^0; \Sigma_b^0) + \mathcal{M}(\rho^+, \Lambda_b^0; \Lambda_b^0) \\
& + \mathcal{M}(K^+, \Xi_b^0; K^{*+}) + \mathcal{M}(K^+, \Xi_b^0; K^{*+}) + \mathcal{M}(K^{*+}, \Xi_b^0; K^+) \\
& + \mathcal{M}(K^{*+}, \Xi_b^0; K^+) + \mathcal{M}(K^+, \Xi_b^0; \Xi_b^0) \\
& + \mathcal{M}(K^+, \Xi_b^0; \Xi_b^0) + \mathcal{M}(K^+, \Xi_b^0; \Xi_b^0) \\
& + \mathcal{M}(K^+, \Xi_b^0; \Xi_b^0) + \mathcal{M}(K^{*+}, \Xi_b^0; \Xi_b^0) \\
& + \mathcal{M}(K^{*+}, \Xi_b^0; \Xi_b^0) + \mathcal{M}(K^{*+}, \Xi_b^0; \Xi_b^0), \quad (\text{B27})
\end{aligned}$$

$$\begin{aligned}
\mathcal{A}(\Xi_{bc}^+ \rightarrow \Sigma_b^+ \bar{K}^0) &= C_{SD}(\Xi_{bc}^+ \rightarrow \Sigma_b^+ \bar{K}^0) + \mathcal{M}(\pi^+, \Xi_b^0; K^{*+}) \\
& + \mathcal{M}(\pi^+, \Xi_b^0; K^{*+}) + \mathcal{M}(\rho^+, \Xi_b^0; K^+) + \mathcal{M}(\rho^+, \Xi_b^0; K^+) \\
& + \mathcal{M}(\pi^+, \Xi_b^0; \Sigma_b^0) + \mathcal{M}(\pi^+, \Xi_b^0; \Lambda_b^0) + \mathcal{M}(\pi^+, \Xi_b^0; \Sigma_b^0) \\
& + \mathcal{M}(\pi^+, \Xi_b^0; \Lambda_b^0) + \mathcal{M}(\rho^+, \Xi_b^0; \Sigma_b^0) \\
& + \mathcal{M}(\rho^+, \Xi_b^0; \Lambda_b^0) + \mathcal{M}(\rho^+, \Xi_b^0; \Sigma_b^0) \\
& + \mathcal{M}(\rho^+, \Xi_b^0; \Lambda_b^0), \quad (\text{B28})
\end{aligned}$$

$$\begin{aligned}
\mathcal{A}(\Xi_{bc}^+ \rightarrow \Sigma_b^+ K^0) &= C_{SD}(\Xi_{bc}^+ \rightarrow \Sigma_b^+ K^0) + \mathcal{M}(K^{*+}, \Lambda_b^0; \pi^+) \\
& + \mathcal{M}(K^{*+}, \Sigma_b^0; \pi^+) + \mathcal{M}(K^+, \Lambda_b^0; \rho^+) \\
& + \mathcal{M}(K^+, \Sigma_b^0; \rho^+) \\
& + \mathcal{M}(K^+, \Lambda_b^0; \Xi_b^0) + \mathcal{M}(K^+, \Lambda_b^0; \Xi_b^0) \\
& + \mathcal{M}(K^+, \Sigma_b^0; \Xi_b^0) + \mathcal{M}(K^+, \Sigma_b^0; \Xi_b^0) \\
& + \mathcal{M}(K^{*+}, \Lambda_b^0; \Xi_b^0)
\end{aligned}$$

$$\begin{aligned}
& + \mathcal{M}(K^{*+}, \Lambda_b^0; \Xi_b^0) + \mathcal{M}(K^{*+}, \Sigma_b^0; \Xi_b^0) \\
& + \mathcal{M}(K^{*+}, \Sigma_b^0; \Xi_b^0), \quad (\text{B29})
\end{aligned}$$

$$\begin{aligned}
\mathcal{A}(\Xi_{bc}^+ \rightarrow \Sigma_b^+ \pi^0) &= C_{SD}(\Xi_{bc}^+ \rightarrow \Sigma_b^+ \pi^0) + \mathcal{M}(\pi^+, \Lambda_b^0; \rho^+) + \mathcal{M}(\pi^+, \Sigma_b^0; \rho^+) \\
& + \mathcal{M}(\rho^+, \Lambda_b^0; \pi^+) + \mathcal{M}(\rho^+, \Sigma_b^0; \pi^+) \\
& + \mathcal{M}(\pi^+, \Lambda_b^0; \Sigma^+) + \mathcal{M}(\pi^+, \Sigma_b^0; \Lambda^+) + \mathcal{M}(\rho^+, \Lambda_b^0; \Sigma^+) \\
& + \mathcal{M}(\rho^+, \Sigma_b^0; \Lambda^+) + \mathcal{M}(K^+, \Xi_b^0; K^{*+}) \\
& + \mathcal{M}(K^+, \Xi_b^0; K^{*+}) + \mathcal{M}(K^{*+}, \Xi_b^0; K^+) + \mathcal{M}(K^{*+}, \Xi_b^0; K^+) \\
& + \mathcal{M}(K^+, \Xi_b^0; \Xi_b^0) + \mathcal{M}(K^+, \Xi_b^0; \Xi_b^0) \\
& + \mathcal{M}(K^+, \Xi_b^0; \Xi_b^0) + \mathcal{M}(K^+, \Xi_b^0; \Xi_b^0) \\
& + \mathcal{M}(K^{*+}, \Xi_b^0; \Xi_b^0) + \mathcal{M}(K^{*+}, \Xi_b^0; \Xi_b^0) + \mathcal{M}(K^{*+}, \Xi_b^0; \Xi_b^0) \\
& + \mathcal{M}(K^{*+}, \Xi_b^0; \Xi_b^0), \quad (\text{B30})
\end{aligned}$$

$$\begin{aligned}
\mathcal{A}(\Xi_{bc}^+ \rightarrow \Xi_b^0 K^+) &= \mathcal{T}(\Xi_{bc}^+ \rightarrow \Xi_b^0 K^+) + \mathcal{M}(K^+, \Xi_b^0; \rho^0) + \mathcal{M}(K^+, \Xi_b^0; \omega) \\
& + \mathcal{M}(K^+, \Xi_b^0; \rho^0) + \mathcal{M}(K^+, \Xi_b^0; \omega) \\
& + \mathcal{M}(K^{*+}, \Xi_b^0; \pi^0) + \mathcal{M}(K^{*+}, \Xi_b^0; \eta_8) \\
& + \mathcal{M}(K^{*+}, \Xi_b^0; \pi^0) + \mathcal{M}(K^{*+}, \Xi_b^0; \eta_8) + \mathcal{M}(\pi^+, \Lambda_b^0; \bar{K}^{*0}) \\
& + \mathcal{M}(\pi^+, \Sigma_b^0; \bar{K}^{*0}) + \mathcal{M}(\rho^+, \Lambda_b^0; \bar{K}^0) \\
& + \mathcal{M}(\rho^+, \Sigma_b^0; \bar{K}^0) + \mathcal{M}(K^+, \Xi_b^0; \phi) \\
& + \mathcal{M}(K^+, \Xi_b^0; \phi) \\
& + \mathcal{M}(K^+, \Xi_b^0; \Omega_b^-) + \mathcal{M}(K^+, \Xi_b^0; \Omega_b^-) \\
& + \mathcal{M}(K^{*+}, \Xi_b^0; \Omega_b^-) + \mathcal{M}(K^{*+}, \Xi_b^0; \Omega_b^-) \\
& + \mathcal{M}(\pi^+, \Lambda_b^0; \Xi_b^-) \\
& + \mathcal{M}(\pi^+, \Lambda_b^0; \Xi_b'^-) + \mathcal{M}(\pi^+, \Sigma_b^0; \Xi_b^-) \\
& + \mathcal{M}(\pi^+, \Sigma_b^0; \Xi_b'^-) + \mathcal{M}(\rho^+, \Lambda_b^0; \Xi_b^-) \\
& + \mathcal{M}(\rho^+, \Lambda_b^0; \Xi_b'^-) \\
& + \mathcal{M}(\rho^+, \Sigma_b^0; \Xi_b^-) + \mathcal{M}(\rho^+, \Sigma_b^0; \Xi_b'^-), \quad (\text{B31})
\end{aligned}$$

$$\begin{aligned}
\mathcal{A}(\Xi_{bc}^+ \rightarrow \Xi_b^0 \pi^+) &= \mathcal{T}(\Xi_{bc}^+ \rightarrow \Xi_b^0 \pi^+) + \mathcal{M}(\pi^+, \Xi_b^0; \rho^0) \\
& + \mathcal{M}(\pi^+, \Xi_b^0; \rho^0) + \mathcal{M}(\rho^+, \Xi_b^0; \pi^0) \\
& + \mathcal{M}(\rho^+, \Xi_b^0; \pi^0) \\
& + \mathcal{M}(\pi^+, \Xi_b^0; \Xi_b^-) + \mathcal{M}(\pi^+, \Xi_b^0; \Xi_b'^-) \\
& + \mathcal{M}(\pi^+, \Xi_b^0; \Xi_b^-) + \mathcal{M}(\pi^+, \Xi_b^0; \Xi_b'^-) \\
& + \mathcal{M}(\rho^+, \Xi_b^0; \Xi_b^-) \\
& + \mathcal{M}(\rho^+, \Xi_b^0; \Xi_b'^-) + \mathcal{M}(\rho^+, \Xi_b^0; \Xi_b^-) \\
& + \mathcal{M}(\rho^+, \Xi_b^0; \Xi_b'^-), \quad (\text{B32})
\end{aligned}$$

$$\begin{aligned}
\mathcal{A}(\Xi_{bc}^0 \rightarrow \Omega_b^- K^+) &= \mathcal{M}(\pi^+, \Xi_b^-; \bar{K}^{*0}) + \mathcal{M}(\pi^+, \Xi_b^-; \bar{K}^{*0}) \\
& + \mathcal{M}(\rho^+, \Xi_b^-; \bar{K}^0) + \mathcal{M}(\rho^+, \Xi_b^-; \bar{K}^0), \quad (\text{B33})
\end{aligned}$$

$$\begin{aligned}
\mathcal{A}(\Xi_{bc}^0 \rightarrow \Sigma_b^0 \eta_8) &= C_{SD}(\Xi_{bc}^0 \rightarrow \Sigma_b^0 \eta_8) \\
& + \mathcal{M}(K^+, \Xi_b^-; K^{*+}) + \mathcal{M}(K^+, \Xi_b'^-; K^{*+}) \\
& + \mathcal{M}(K^{*+}, \Xi_b^-; K^+) + \mathcal{M}(K^{*+}, \Xi_b'^-; K^+) \\
& + \mathcal{M}(K^+, \Xi_b^-; \Xi_b^-) + \mathcal{M}(K^+, \Xi_b'^-; \Xi_b^-) \\
& + \mathcal{M}(K^+, \Xi_b^-; \Xi_b^-) + \mathcal{M}(K^+, \Xi_b'^-; \Xi_b^-) \\
& + \mathcal{M}(K^{*+}, \Xi_b^-; \Xi_b^-) \\
& + \mathcal{M}(K^{*+}, \Xi_b^-; \Xi_b'^-) + \mathcal{M}(K^{*+}, \Xi_b'^-; \Xi_b^-) \\
& + \mathcal{M}(K^{*+}, \Xi_b'^-; \Xi_b'^-) + \mathcal{M}(\pi^+, \Sigma_b^-; \Sigma_b^-) \\
& + \mathcal{M}(\rho^+, \Sigma_b^-; \Sigma_b^-), \quad (\text{B34})
\end{aligned}$$

$$\begin{aligned}
\mathcal{A}(\Xi_{bc}^0 \rightarrow \Sigma_b^0 \bar{K}^0) &= C_{SD}(\Xi_{bc}^0 \rightarrow \Sigma_b^0 \bar{K}^0) + \mathcal{M}(\pi^+, \Xi_b^-; K^{*+}) \\
& + \mathcal{M}(\pi^+, \Xi_b^-; K^{*+}) + \mathcal{M}(\rho^+, \Xi_b^-; K^+) + \mathcal{M}(\rho^+, \Xi_b^-; K^+) \\
& + \mathcal{M}(\pi^+, \Xi_b^-; \Sigma_b^-) + \mathcal{M}(\pi^+, \Xi_b'^-; \Sigma_b^-) \\
& + \mathcal{M}(\rho^+, \Xi_b^-; \Sigma_b^-) + \mathcal{M}(\rho^+, \Xi_b'^-; \Sigma_b^-), \quad (\text{B35})
\end{aligned}$$

$$\mathcal{A}(\Xi_{bc}^0 \rightarrow \Sigma_b^0 K^0) = C_{SD}(\Xi_{bc}^0 \rightarrow \Sigma_b^0 K^0) + \mathcal{M}(K^+, \Sigma_b^-; \rho^+) + \mathcal{M}(K^{*+}, \Sigma_b^-; \pi^+)$$

$$\begin{aligned}
& + \mathcal{M}(\rho^+, \Xi_b^{\prime-}; \pi^0) \\
& + \mathcal{M}(K^+, \Omega_b^-; K^{*0}) + \mathcal{M}(K^{*+}, \Omega_b^-; K^0), \quad (\text{B54})
\end{aligned}$$

$$\begin{aligned}
\mathcal{A}(\Omega_{bc}^0 \rightarrow \Xi_b^0 \eta_8) = & C_{SD}(\Omega_{bc}^0 \rightarrow \Xi_b^0 \eta_8) + \mathcal{M}(K^+, \Omega_b^-; K^{*+}) \\
& + \mathcal{M}(K^{*+}, \Omega_b^-; K^+) + \mathcal{M}(K^+, \Omega_b^-; \Omega_b^-) + \mathcal{M}(K^{*+}, \Omega_b^-; \Omega_b^-) \\
& + \mathcal{M}(\pi^+, \Xi_b^-; \Xi_b^-) + \mathcal{M}(\pi^+, \Xi_b^-; \Xi_b^{\prime-}) \\
& + \mathcal{M}(\pi^+, \Xi_b^-; \Xi_b^-) + \mathcal{M}(\pi^+, \Xi_b^-; \Xi_b^{\prime-}) + \mathcal{M}(\rho^+, \Xi_b^-; \Xi_b^-) \\
& + \mathcal{M}(\rho^+, \Xi_b^-; \Xi_b^{\prime-}) + \mathcal{M}(\rho^+, \Xi_b^-; \Xi_b^-) \\
& + \mathcal{M}(\rho^+, \Xi_b^-; \Xi_b^{\prime-}) + \mathcal{M}(\pi^+, \Xi_b^-; \rho^+) \\
& + \mathcal{M}(\pi^+, \Xi_b^-; \rho^+) \\
& + \mathcal{M}(\rho^+, \Xi_b^-; \pi^+) + \mathcal{M}(\rho^+, \Xi_b^-; \pi^+), \quad (\text{B55})
\end{aligned}$$

$$\begin{aligned}
\mathcal{A}(\Omega_{bc}^0 \rightarrow \Xi_b^0 \bar{K}^0) = & C_{SD}(\Omega_{bc}^0 \rightarrow \Xi_b^0 \bar{K}^0) + \mathcal{M}(\pi^+, \Omega_b^-; K^{*+}) \\
& + \mathcal{M}(\rho^+, \Omega_b^-; K^+) + \mathcal{M}(\pi^+, \Omega_b^-; \Xi_b^-) + \mathcal{M}(\pi^+, \Omega_b^-; \Xi_b^{\prime-}) \\
& + \mathcal{M}(\rho^+, \Omega_b^-; \Xi_b^-) + \mathcal{M}(\rho^+, \Omega_b^-; \Xi_b^{\prime-}), \quad (\text{B56})
\end{aligned}$$

$$\begin{aligned}
\mathcal{A}(\Omega_{bc}^0 \rightarrow \Xi_b^0 K^0) = & C_{SD}(\Omega_{bc}^0 \rightarrow \Xi_b^0 K^0) \\
& + \mathcal{M}(K^+, \Xi_b^-; \rho^+) + \mathcal{M}(K^+, \Xi_b^-; \rho^+) + \mathcal{M}(K^{*+}, \Xi_b^-; \pi^+) \\
& + \mathcal{M}(K^{*+}, \Xi_b^-; \pi^+) \\
& + \mathcal{M}(K^+, \Xi_b^-; \Omega_b^-) + \mathcal{M}(K^+, \Xi_b^-; \Omega_b^-) \\
& + \mathcal{M}(K^{*+}, \Xi_b^-; \Omega_b^-) + \mathcal{M}(K^{*+}, \Xi_b^-; \Omega_b^-), \quad (\text{B57})
\end{aligned}$$

$$\begin{aligned}
\mathcal{A}(\Omega_{bc}^0 \rightarrow \Xi_b^0 \pi^0) = & C_{SD}(\Omega_{bc}^0 \rightarrow \Xi_b^0 \pi^0) + \mathcal{M}(\pi^+, \Xi_b^-; \rho^+) \\
& + \mathcal{M}(\pi^+, \Xi_b^-; \rho^+) + \mathcal{M}(\rho^+, \Xi_b^-; \pi^+) \\
& + \mathcal{M}(\rho^+, \Xi_b^-; \pi^+) \\
& + \mathcal{M}(K^+, \Omega_b^-; K^{*+}) + \mathcal{M}(K^{*+}, \Omega_b^-; K^+) \\
& + \mathcal{M}(\pi^+, \Xi_b^-; \Xi_b^-) + \mathcal{M}(\pi^+, \Xi_b^-; \Xi_b^{\prime-}) \\
& + \mathcal{M}(\pi^+, \Xi_b^-; \Xi_b^-) \\
& + \mathcal{M}(\pi^+, \Xi_b^-; \Xi_b^{\prime-}) + \mathcal{M}(\rho^+, \Xi_b^-; \Xi_b^-) \\
& + \mathcal{M}(\rho^+, \Xi_b^-; \Xi_b^{\prime-}) + \mathcal{M}(\rho^+, \Xi_b^-; \Xi_b^-) \\
& + \mathcal{M}(\rho^+, \Xi_b^-; \Xi_b^{\prime-}). \quad (\text{B58})
\end{aligned}$$

References

- R. Aaij, et al., [LHCb Collaboration], Observation of the doubly charmed baryon Ξ_{cc}^{++} . Phys. Rev. Lett. **119**(11), 112001 (2017). [arXiv:1707.01621](#) [hep-ex]
- R. Aaij, et al. [LHCb Collaboration], First Observation of the Doubly Charmed Baryon Decay $\Xi_{cc}^{++} \rightarrow \Xi_c^+ \pi^+$. Phys. Rev. Lett. **121**(16), 162002 (2018). [arXiv:1807.01919](#) [hep-ex]
- A. De Rujula, H. Georgi, S.L. Glashow, Hadron masses in a gauge theory. Phys. Rev. D **12**, 147 (1975)
- R.L. Jaffe, J.E. Kiskis, Spectra of new hadrons. Phys. Rev. D **13**, 1355 (1976)
- W. Ponce, Heavy quarks in a spherical bag. Phys. Rev. D **19**, 2197 (1979)
- F.S. Yu, H.Y. Jiang, R.H. Li, C.D. Lü, W. Wang, Z.X. Zhao, Discovery potentials of doubly charmed baryons. Chin. Phys. C **42**(5), 051001 (2018). [arXiv:1703.09086](#) [hep-ph]
- F.S. Yu, Role of decay in the search for double-charm baryons. Sci. China Phys. Mech. Astron. **63**(2), 221065 (2020). [arXiv:1912.10253](#) [hep-ex]
- J.J. Han, H.Y. Jiang, W. Liu, Z.J. Xiao, F.S. Yu, Rescattering mechanism of weak decays of double-charm baryons. [arXiv:2101.12019](#) [hep-ph]
- H.Y. Cheng, C.W. Chiang, Two-body hadronic charmed meson decays. Phys. Rev. D **81**, 074021 (2010). [arXiv:1001.0987](#) [hep-ph]
- Hn Li, C.D. Lü, F.S. Yu, Branching ratios and direct CP asymmetries in $D \rightarrow PP$ decays. Phys. Rev. D **86**, 036012 (2012). [arXiv:1203.3120](#) [hep-ph]
- Hn Li, C.D. Lü, Q. Qin, F.S. Yu, Branching ratios and direct CP asymmetries in $D \rightarrow PV$ decays. Phys. Rev. D **89**(5), 054006 (2014). [arXiv:1305.7021](#) [hep-ph]
- C.D. Lü, W. Wang, F.S. Yu, Test flavor SU(3) symmetry in exclusive Λ_c decays. Phys. Rev. D **93**(5), 056008 (2016). [arXiv:1601.04241](#) [hep-ph]
- C.Q. Geng, Y.K. Hsiao, Y.H. Lin, L.L. Liu, Non-leptonic two-body weak decays of Λ_c (2286). Phys. Lett. B **776**, 265–269 (2018). [arXiv:1708.02460](#) [hep-ph]
- C.Q. Geng, Y.K. Hsiao, C.W. Liu, T.H. Tsai, Charmed baryon weak decays with SU(3) flavor symmetry. JHEP **11**, 147 (2017). [arXiv:1709.00808](#) [hep-ph]
- D. Wang, P.F. Guo, W.H. Long, F.S. Yu, $K_S^0 - K_L^0$ asymmetries and CP violation in charmed baryon decays into neutral kaons. JHEP **03**, 066 (2018). [arXiv:1709.09873](#) [hep-ph]
- C.Q. Geng, Y.K. Hsiao, C.W. Liu, T.H. Tsai, Antitriplet charmed baryon decays with SU(3) flavor symmetry. Phys. Rev. D **97**(7), 073006 (2018). [arXiv:1801.03276](#) [hep-ph]
- H.Y. Cheng, X.W. Kang, F. Xu, Singly Cabibbo-suppressed hadronic decays of Λ_c^+ . Phys. Rev. D **97**(7), 074028 (2018). [arXiv:1801.08625](#) [hep-ph]
- H.Y. Jiang, F.S. Yu, Fragmentation-fraction ratio f_{Ξ_b}/f_{Λ_b} in b - and c -baryon decays. Eur. Phys. J. C **78**(3), 224 (2018). [arXiv:1802.02948](#) [hep-ph]
- Z.X. Zhao, Weak decays of heavy baryons in the light-front approach. Chin. Phys. C **42**(9), 093101 (2018). [arXiv:1803.02292](#) [hep-ph]
- C.Q. Geng, Y.K. Hsiao, C.W. Liu, T.H. Tsai, SU(3) symmetry breaking in charmed baryon decays. Eur. Phys. J. C **78**(7), 593 (2018). [arXiv:1804.01666](#) [hep-ph]
- C.Q. Geng, Y.K. Hsiao, C.W. Liu, T.H. Tsai, Three-body charmed baryon Decays with SU(3) flavor symmetry. Phys. Rev. D **99**(7), 073003 (2019). [arXiv:1810.01079](#) [hep-ph]
- X.G. He, Y.J. Shi, W. Wang, Unification of flavor SU(3) analyses of heavy hadron weak decays. Eur. Phys. J. C **80**(5), 359 (2020). [arXiv:1811.03480](#) [hep-ph]
- H.J. Zhao, Y.L. Wang, Y.K. Hsiao, Y. Yu, A diagrammatic analysis of two-body charmed baryon decays with flavor symmetry. JHEP **02**, 165 (2020). [arXiv:1811.07265](#) [hep-ph]
- Y. Grossman, S. Schacht, U-spin sum rules for CP asymmetries of three-body charmed baryon decays. Phys. Rev. D **99**(3), 033005 (2019). [arXiv:1811.11188](#) [hep-ph]
- C.Q. Geng, C.W. Liu, T.H. Tsai, Singly Cabibbo suppressed decays of Λ_c^+ with SU(3) flavor symmetry. Phys. Lett. B **790**, 225–228 (2019). [arXiv:1812.08508](#) [hep-ph]
- D. Wang, Sum rules for CP asymmetries of charmed baryon decays in the $SU(3)_F$ limit. Eur. Phys. J. C **79**(5), 429 (2019). [arXiv:1901.01776](#) [hep-ph]
- C.Q. Geng, C.W. Liu, T.H. Tsai, Asymmetries of anti-triplet charmed baryon decays. Phys. Lett. B **794**, 19–28 (2019). [arXiv:1902.06189](#) [hep-ph]
- Y.K. Hsiao, Y. Yao, H.J. Zhao, Two-body charmed baryon decays involving vector meson with SU(3) flavor symmetry. Phys. Lett. B **792**, 35–39 (2019). [arXiv:1902.08783](#) [hep-ph]
- C.Q. Geng, C.W. Liu, T.H. Tsai, Y. Yu, Charmed baryon weak decays with Decuplet baryon and SU(3) flavor symmetry. Phys. Rev. D **99**(11), 114022 (2019). [arXiv:1904.11271](#) [hep-ph]
- C.P. Jia, D. Wang, F.S. Yu, Charmed baryon decays in $SU(3)_F$ symmetry. Nucl. Phys. B **956**, 115048 (2020). [arXiv:1910.00876](#) [hep-ph]

31. J. Zou, F. Xu, G. Meng, H.Y. Cheng, Two-body hadronic weak decays of antitriplet charmed baryons. *Phys. Rev. D* **101**(1), 014011 (2020). [arXiv:1910.13626](#) [hep-ph]
32. C.Q. Geng, C.W. Liu, T.H. Tsai, Charmed baryon weak decays with vector mesons. *Phys. Rev. D* **101**(5), 053002 (2020). [arXiv:2001.05079](#) [hep-ph]
33. P.Y. Niu, J.M. Richard, Q. Wang, Q. Zhao, Hadronic weak decays of Λ_c in the quark model. *Phys. Rev. D* **102**(7), 073005 (2020). [arXiv:2003.09323](#) [hep-ph]
34. Y.K. Hsiao, Q. Yi, S.T. Cai, H.J. Zhao, Two-body charmed baryon decays involving Decuplet baryon in the quark-diagram scheme. *Eur. Phys. J. C* **80**(11), 1067 (2020). [arXiv:2006.15291](#) [hep-ph]
35. J. Pan, Y.K. Hsiao, J. Sun, X.G. He, $SU(3)$ flavor symmetry for weak hadronic decays of B_{bc} baryons. *Phys. Rev. D* **102**(5), 056005 (2020). [arXiv:2007.02504](#) [hep-ph]
36. G. Meng, S.M.Y. Wong, F. Xu, Doubly Cabibbo-suppressed decays of antitriplet charmed baryons. *JHEP* **11**, 126 (2020). [arXiv:2005.12111](#) [hep-ph]
37. S. Hu, G. Meng, F. Xu, Hadronic weak decays of the charmed baryon Ω_c . *Phys. Rev. D* **101**(9), 094033 (2020). [arXiv:2003.04705](#) [hep-ph]
38. H.Y. Cheng, Phenomenological study of heavy hadron lifetimes. *JHEP* **11**, 014 (2018). [arXiv:1807.00916](#) [hep-ph]
39. R.H. Li, C.D. Lü, W. Wang, F.S. Yu, Z.T. Zou, Doubly-heavy baryon weak decays: $\Xi_{bc}^0 \rightarrow pK^-$ and $\Xi_{bc}^+ \rightarrow \Sigma_c^{++}(2520)K^-$. *Phys. Lett. B* **767**, 232–235 (2017). [arXiv:1701.03284](#) [hep-ph]
40. L.J. Jiang, B. He, R.H. Li, Weak decays of doubly heavy baryons: $B_{cc} \rightarrow B_c V$. *Eur. Phys. J. C* **78**(11), 961 (2018). [arXiv:1810.00541](#) [hep-ph]
41. R.H. Li, J.J. Hou, B. He, Y.R. Wang, Weak decays of doubly heavy baryons: $B_{cc} \rightarrow \mathcal{B}D^{(*)}$. [arXiv:2010.09362](#) [hep-ph]
42. D.A. Egolf, R.P. Springer, J. Urban, $SU(3)$ predictions for weak decays of doubly heavy baryons including $SU(3)$ breaking terms. *Phys. Rev. D* **68**, 013003 (2003). [arXiv:hep-ph/0211360](#)
43. Y.J. Shi, W. Wang, Y. Xing, J. Xu, Weak decays of doubly heavy baryons: multi-body decay channels. *Eur. Phys. J. C* **78**(1), 56 (2018). [arXiv:1712.03830](#) [hep-ph]
44. A.I. Onishchenko, Inclusive and exclusive decays of doubly heavy baryons. [arXiv:hep-ph/0006295](#)
45. W. Wang, F.S. Yu, Z.X. Zhao, Weak decays of doubly heavy baryons: the $1/2 \rightarrow 1/2$ case. *Eur. Phys. J. C* **77**(11), 781 (2017). [arXiv:1707.02834](#) [hep-ph]
46. Q.A. Zhang, Weak decays of doubly heavy baryons: W-exchange. *Eur. Phys. J. C* **78**(12), 1024 (2018). [arXiv:1811.02199](#) [hep-ph]
47. W. Wang, Z.P. Xing, J. Xu, Weak decays of doubly heavy baryons: $SU(3)$ analysis. *Eur. Phys. J. C* **77**(11), 800 (2017). [arXiv:1707.06570](#) [hep-ph]
48. H.Y. Cheng, G. Meng, F. Xu, J. Zou, Two-body weak decays of doubly charmed baryons. *Phys. Rev. D* **101**(3), 034034 (2020). [arXiv:2001.04553](#) [hep-ph]
49. H.Y. Cheng, F. Xu, Lifetimes of doubly heavy baryons B_{bb} and B_{bc} . *Phys. Rev. D* **99**(7), 073006 (2019). [arXiv:1903.08148](#) [hep-ph]
50. H.Y. Cheng, Y.L. Shi, Lifetimes of doubly charmed baryons. *Phys. Rev. D* **98**(11), 113005 (2018). [arXiv:1809.08102](#) [hep-ph]
51. Y.J. Shi, W. Wang, Z.X. Zhao, QCD sum rules analysis of weak decays of doubly-heavy baryons. *Eur. Phys. J. C* **80**(6), 568 (2020). [arXiv:1902.01092](#) [hep-ph]
52. T. Gutsche, M.A. Ivanov, J.G. Körner, V.E. Lyubovitskij, Decay chain information on the newly discovered double charm baryon state Ξ_{cc}^{++} . *Phys. Rev. D* **96**(5), 054013 (2017). [arXiv:1708.00703](#) [hep-ph]
53. X.H. Hu, Y.L. Shen, W. Wang, Z.X. Zhao, Weak decays of doubly heavy baryons: “decay constants”. *Chin. Phys. C* **42**(12), 123102 (2018). [arXiv:1711.10289](#) [hep-ph]
54. Z.X. Zhao, Weak decays of doubly heavy baryons: the $1/2 \rightarrow 3/2$ case. *Eur. Phys. J. C* **78**(9), 756 (2018). [arXiv:1805.10878](#) [hep-ph]
55. Z.P. Xing, Z.X. Zhao, Weak decays of doubly heavy baryons: the FCNC processes. *Phys. Rev. D* **98**(5), 056002 (2018). [arXiv:1807.03101](#) [hep-ph]
56. R. Dhir, N. Sharma, Weak decays of doubly heavy charm Ω_{cc}^+ baryon. *Eur. Phys. J. C* **78**(9), 743 (2018)
57. Y.J. Shi, Y. Xing, Z.X. Zhao, Light-cone sum rules analysis of $\Xi_{QQ'q} \rightarrow \Lambda_{Q'}$ weak decays. *Eur. Phys. J. C* **79**(6), 501 (2019). [arXiv:1903.03921](#) [hep-ph]
58. Y. Xing, F.S. Yu, R. Zhu, Weak decays of stable open-bottom tetraquark by $SU(3)$ symmetry analysis. *Eur. Phys. J. C* **79**(5), 373 (2019). [arXiv:1903.05973](#) [hep-ph]
59. T. Gutsche, M.A. Ivanov, J.G. Körner, V.E. Lyubovitskij, Novel ideas in nonleptonic decays of double heavy baryons. *Particles* **2**(2), 339–356 (2019). [arXiv:1905.06219](#) [hep-ph]
60. X.H. Hu, Y.J. Shi, Light-cone sum rules analysis of $\Xi_{QQ'} \rightarrow \Sigma_{Q'}$ weak decays. *Eur. Phys. J. C* **80**(1), 56 (2020). [arXiv:1910.07909](#) [hep-ph]
61. T. Gutsche, M.A. Ivanov, J.G. Körner, V.E. Lyubovitskij, Z. Tyulemissov, Analysis of the semileptonic and nonleptonic two-body decays of the double heavy charm baryon states Ξ_{cc}^{++} , Ξ_{cc}^+ and Ω_{cc}^+ . *Phys. Rev. D* **100**(11), 114037 (2019). [arXiv:1911.10785](#) [hep-ph]
62. H.W. Ke, F. Lu, X.H. Liu, X.Q. Li, Study on $\Xi_{cc} \rightarrow \Xi_c$ and $\Xi_{cc} \rightarrow \Xi_c'$ weak decays in the light-front quark model. *Eur. Phys. J. C* **80**(2), 140 (2020). [arXiv:1912.01435](#) [hep-ph]
63. X.H. Hu, R.H. Li, Z.P. Xing, A comprehensive analysis of weak transition form factors for doubly heavy baryons in the light front approach. *Eur. Phys. J. C* **80**(4), 320 (2020). [arXiv:2001.06375](#) [hep-ph]
64. Y.J. Shi, W. Wang, Z.X. Zhao, U.G. Meißner, Towards a heavy diquark effective theory for weak decays of doubly heavy baryons. *Eur. Phys. J. C* **80**(5), 398 (2020). [arXiv:2002.02785](#) [hep-ph]
65. M.A. Ivanov, J.G. Körner, V.E. Lyubovitskij, Nonleptonic decays of doubly charmed baryons. *Phys. Part. Nucl.* **51**(4), 678–685 (2020)
66. A.K. Leibovich, Z. Ligeti, I.W. Stewart, M.B. Wise, Predictions for nonleptonic Λ_b and Θ_b decays. *Phys. Lett. B* **586**, 337 (2004). [arXiv:hep-ph/0312319](#)
67. S. Mantry, D. Pirjol, I.W. Stewart, Strong phases and factorization for color suppressed decays. *Phys. Rev. D* **68**, 114009 (2003). [arXiv:hep-ph/0306254](#)
68. H.Y. Cheng, C.K. Chua, A. Soni, Final state interactions in hadronic B decays. *Phys. Rev. D* **71**, 014030 (2005). [arXiv:hep-ph/0409317](#)
69. Q.X. Yu, X.H. Guo, Masses of doubly heavy baryons in the Bethe–Salpeter equation approach. *Nucl. Phys. B* **947**, 114727 (2019). [arXiv:1810.00437](#) [hep-ph]
70. A.V. Berezhnoy, A.K. Likhoded, A.V. Luchinsky, Doubly heavy baryons at the LHC. *Phys. Rev. D* **98**(11), 113004 (2018). [arXiv:1809.10058](#) [hep-ph]
71. P.A. Zyla et al., [Particle Data Group], *PTEP* **2020**(8), 083C01 (2020)
72. H.M. Choi, C.R. Ji, Z. Li, H.Y. Ryu, Variational analysis of mass spectra and decay constants for ground state pseudoscalar and vector mesons in the light-front quark model. *Phys. Rev. C* **92**(5), 055203 (2015). [arXiv:1502.03078](#) [hep-ph]
73. T. Feldmann, P. Kroll, B. Stech, Mixing and decay constants of pseudoscalar mesons. *Phys. Rev. D* **58**, 114006 (1998). [arXiv:hep-ph/9802409](#)
74. T.M. Yan, H.Y. Cheng, C.Y. Cheung, G.L. Lin, Y.C. Lin, H.L. Yu, Heavy quark symmetry and chiral dynamics. *Phys. Rev. D* **46**, 1148 (1992). (Erratum: [*Phys. Rev. D* **55**, 5851 (1997)])
75. R. Casalbuoni, A. Deandrea, N. Di Bartolomeo, R. Gatto, F. Feruglio, G. Nardulli, Phenomenology of heavy meson chiral Lagrangians. *Phys. Rep.* **281**, 145 (1997). [arXiv:hep-ph/9605342](#)
76. U.G. Meißner, Low-energy hadron physics from effective chiral Lagrangians with vector mesons. *Phys. Rep.* **161**, 213 (1988)

77. N. Li, S.L. Zhu, Hadronic molecular states composed of heavy flavor baryons. *Phys. Rev. D* **86**, 014020 (2012). [arXiv:1204.3364](#) [hep-ph]
78. T.M. Aliev, K. Azizi, M. Savci, Strong coupling constants of light pseudoscalar mesons with heavy baryons in QCD. *Phys. Lett. B* **696**, 220 (2011). [arXiv:1009.3658](#) [hep-ph]
79. T.M. Aliev, K. Azizi, M. Savci, Heavy baryon-light vector meson couplings in QCD. *Nucl. Phys. A* **852**, 141 (2011). [arXiv:1011.0086](#) [hep-ph]
80. A. Ali, G. Kramer, C.D. Lu, Experimental tests of factorization in charmless nonleptonic two-body B decays. *Phys. Rev. D* **58**, 094009 (1998). [arXiv:hep-ph/9804363](#)
81. V.V. Kiselev, A.K. Likhoded, Baryons with two heavy quarks. *Phys. Usp.* **45**, 455–506 (2002). [arXiv:hep-ph/0103169](#)